27759

NATIONAL LIBRARY
OTTAWA

CANADA

BIBLIOTHÈQUE NATIONALE
OTTAWA

NAME OF AUTHOR........Ronald George Wiens
TITLE OF THESIS.......Development of the
Substorm Westward
Electrojet
UNIVERSITY.......Alberta
DEGREE FOR WHICH THESIS WAS PRESENTED.......M.Sc.
YEAR THIS DEGREE GRANTED.......1976

Permission is hereby granted to THE NATIONAL LIBRARY OF CANADA to microfilm this thesis and to lend or sell copies of the film.

The author reserves other publication rights, and neither the thesis nor extensive extracts from it may be printed or otherwise reproduced without the author's written permission.

(Signed).......Ronald Wiens

PERMANENT ADDRESS:
8103 - 169St
EDMONTON

DATED.......April 22.......1976

NL-91 (10-68)

THE UNIVERSITY OF ALBERTA

DEVELOPMENT OF THE SUBSTORM WESTWARD ELECTROJET

RONALD G. WIENS ©

A THESIS

SUBMITTED TO THE FACULTY OF GRADUATE STUDIES AND RESEARCH
IN PARTIAL FULFILMENT OF THE REQUIREMENTS FOR THE DEGREE
OF MASTER OF SCIENCE

DEPARTMENT OF PHYSICS

EDMONTON, ALBERTA

SPRING, 1976

THE UNIVERSITY OF ALBERTA

FACULTY OF GRADUATE STUDIES AND RESEARCH

The undersigned certify that they have read, and recommend to the Faculty of Graduate Studies and Research, for acceptance, a thesis entitled DEVELOPMENT OF THE SUBSTORM WESTWARD ELECTROJET submitted by RONALD G. WIENS in partial fulfilment of the requirements for the degree of Master of Science.

Supervisor

D. D. Betts

Date April 14 1976

ABSTRACT

Using high-, mid- and low-latitude magnetograms it is demonstrated that the westward expansion of the substorm westward electrojet is not continuous but takes place as a series of discrete steps or jumps. The substorm is pictured as consisting of the sequential development of a series of westward electrojets which we have labeled a 'substorm sequence'. The westward electrojets develop in succession at intervals of about 5-15 minutes in such a way that each new electrojet appears to the northwest of the previous one. Each substorm intensification is accompanied by a response in the adjacent sector to the west consistent with the signatures of growth suggested by McPherron (1972) and Iijima and Nagata (1972). It is suggested that growth may be stimulated by the same mechanism which triggers the expansion phase and that the energy responsible for ensuing substorm intensifications in the evening sector is made available in this fashion.

ACKNOWLEDGEMENTS

I thank Dr. G. Rostoker for his support throughout the course of this research. I also wish to thank Dr. J. L. Kisabeth, Dr. D. D. Wallis and Dr. J. V. Olson for useful discussions.

I would like to thank the University of Alberta for the award of their Graduate Fellowship, the Killam Memorial Foundation for the award of the Killam Fellowship and the National Research Council of Canada for the award of a Graduate Scholarship.

TABLE OF CONTENTS

LIST OF TABLES

LIST OF FIGURES

[illegible] 49

[illegible]

[illegible]

[illegible] with [illegible]

2.10 [illegible] horizontal [illegible] perturbation [illegible] the time [illegible] the maximum [illegible] of each [illegible] upper right hand corner [illegible] given the time at which a baseline [illegible] level was chosen (which was just prior to the onset of event B). The dashed line in each of the two plots indicates the estimated position of the central meridian of the westward electrojet associated with event B. The arrow on the outside of the second polar plot indicates the central meridian of the previous electrojet which was associated with event A. 58

Page

CHAPTER I

INTRODUCTION

1.1 Structure of the Magnetosphere

It is now recognized that, in addition to electromagnetic radiation, the sun continually emits a stream of energetic electrons and protons known as the solar wind. At distances of 1 a.u. from the sun, typical solar wind velocities are ~ 300-500 km/sec while number densities are of the order of ~ 5-10/cm³. Under normal circumstances the velocity of the solar wind exceeds both the velocity of sound and the Alfvén velocity in the interplanetary medium. The solar wind carries with it the coronal magnetic field of the sun which is termed the interplanetary magnetic field (IMF). Typical values of the IMF at the orbit of the earth are ~ 5-10 nT, with approximately 80% of this field lying in the ecliptic plane.

The earth acts as an obstacle in the solar wind flow, and the character of the flow in the vicinity of the obstacle can be understood in terms of hydrodynamic and magnetohydrodynamic theory (Spreiter and Alksne, 1969). Although the main magnetic field of the earth is nearly dipolar, the interaction of the solar wind with the earth's magnetic field results in a distortion of the field configuration where the field in front of the earth is compressed while behind the earth it is distended to great distances forming a distended tail (Figure 1.1).

Since the solar wind velocity is both supersonic and super-Alfvénic, a standing magnetohydrodynamic shock wave exists upstream from the boundary between the interior of the earth's magnetic field cavity and the solar wind plasma (Axford, 1962; Kellogg, 1962). The effect of this MHD shock wave is to slow down (and therefore thermalize) the solar wind plasma so that it can flow around the obstacle which the earth's magnetic field configuration represents. The shocked plasma which flows around the magnetic field cavity is called the <u>magnetosheath</u>. A sharp boundary, termed the <u>magnetopause</u> separates the magnetosheath plasma from the region dominated by the earth's main field which is known as the <u>magnetosphere</u>. At the magnetopause boundary, the pressure of the earth's magnetic field balances the dynamic pressure of the shocked solar wind plasma in the magnetosheath. The geomagnetic field has an intensity of ~ 50 nT just inside the magnetopause, with a sharp drop at the boundary to typical magnetosheath values of ~ 10 nT.

The magnetic field of the earth under the sweeping action of the solar wind forms a magnetic tail in the anti-

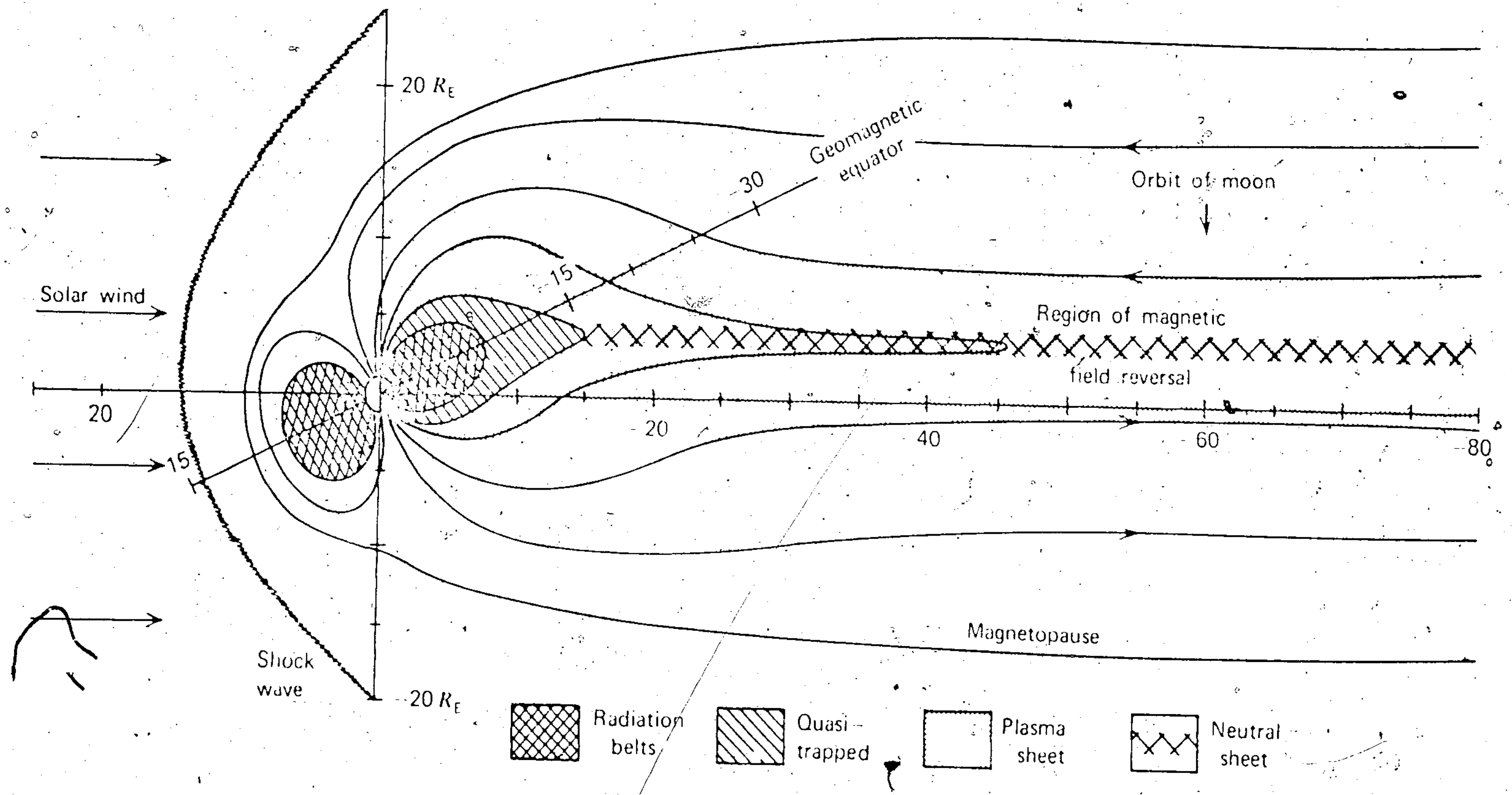
20 R_E
-20 R_E
Solar wind
Shock wave
Geomagnetic equator
30
15
15
20
-20
40
60
-80
Orbit of moon
Region of magnetic field reversal
Magnetopause
Radiation belts
Quasi-trapped
Plasma sheet
Neutral sheet

Figure 1.1

solar direction. Thus behind the earth the magnetopause becomes a cylindrical surface. The radius of the magnetic tail is approximately 22 R_E and remains ~~the~~ same for at least 100 R_E. As seen from Figure 1.1, it is the magnetic field of the polar cap which has been swept back by the solar wind. The incoming field lines in the northern half and the outgoing field lines in the southern half of the magnetic tail are separated by a thin layer where the intensity of the magnetic field drops essentially to zero. This neutral layer has a thickness of about 1000 km and is called the neutral sheet (Ness, 1969).

The magnetic tail of the earth's magnetosphere has been detected with certainty by satellites orbiting the moon so that it definitely extends at least half a million kilometers in the anti-solar direction (Ness et al., 1967a). Mariner 4 (Van Allen, 1965) has found no evidence of the tail at 3,300 R_E, whereas observations with Pioneer 7 near 1000 R_E were rather ambiguous (Ness et al., 1967b).

On both sides of the neutral sheet, satellites have found high fluxes ($10^8 - 10^9$ el $cm^{-2}s^{-1}$) of low energy electrons with energies typically of the order of a few KeV. This region, in which the neutral sheet is embedded, is called the <u>plasma sheet</u> and has a thickness of about 10 R_E (Bame et al., 1967). The plasma sheet starts beyond the termination of the belts of trapped radiation (i.e. beyond the last field lines that maintain their nearly dipole shape as the earth rotates) and has been observed to extend out to at least 100 R_E beyond which no observations have been made.

Close to the earth (3-5 R_E) the particles in the magnetosphere are trapped in the earth's magnetic field. This region of stably trapped particles is called the <u>plasmasphere</u> and the boundary of these stably trapped particles is known as the <u>plasmapause</u>. Just outside the plasmasphere is a region consisting of quasi-trapped particles. The particles in this region are stably trapped on the day side of the earth. However as the particles in this region drift around to the night side of the earth, the earth's magnetic field becomes sufficiently distorted to sometimes allow these particles to escape down field lines into the earth's ionosphere, or out into the magnetotail.

1.2 <u>Magnetospheric Storms</u>

When the sun is active the solar wind interacts with the earth's magnetic field and causes an enhanced level of magnetospheric disturbance. When the disturbance is intense enough, it may be called a <u>magnetospheric storm</u>.

For example a solar plasma stream ejected during an intense solar flare generates a shock wave in the interplanetary plasma. A magnetospheric storm begins when this plasma stream reaches the earth's magnetic field. The initial effect of the shock wave is to compress the magnetosphere. Then, through a process that is not yet fully understood, energy is transferred from the plasma stream to the magnetosphere. This energy is stored temporarily in the tail of the magnetosphere and continues to build up until an interaction occurs between the geomagnetic tail and the ionosphere in which magnetic energy stored in the tail is suddenly released and converted into kinetic energy of the ambient plasma. This explosive release of energy is known as a <u>magnetospheric substorm</u>. It is the integral effect of a whole series of substorms which occur in rapid succession that contributes to the generation of a magnetospheric storm. The lifetime of the individual explosive processes is typically one to three hours, much shorter than the lifetime of a typical magnetospheric storm which is one to three days.

The energy released during a substorm generates many diverse electromagnetic phenomena. The character of these phenomena has been discussed in great detail by Akasofu (1968). He has subdivided the magnetospheric substorm into substorms involving different portions of the electromagnetic spectrum. There are the auroral substorm, the polar magnetic substorm, the ionospheric substorm, the x-ray substorm, the proton aurora substorm, the ULF emission substorm, and the micropulsation substorm. Throughout this thesis we will be primarily interested in the auroral and polar magnetic substorms.

1.3 Auroral Substorms

During a quiet period (namely, the period between two successive substorms) quiet arcs tend to lie along an oval belt known as the auroral oval. The situation is shown in Figure 1.2 in which the average location of the oval is indicated. The auroral oval discussed above is observed during average (moderately quiet) conditions. In periods of extreme quiet the night-time sector of the auroral oval moves up to geomagnetic latitudes of ~ 75° while during great storms this sector has been observed at latitudes below 50°.

Figure 1.3 shows the growth and decay of a canonical auroral substorm (A→B→C→D→E→F→A). The auroral substorm has two characteristic phases; the expansive phase and the recovery phase (Akasofu, 1964). The first indication of the substorm is a sudden brightening of one of the quiet arcs lying in the mid-night sector of the oval

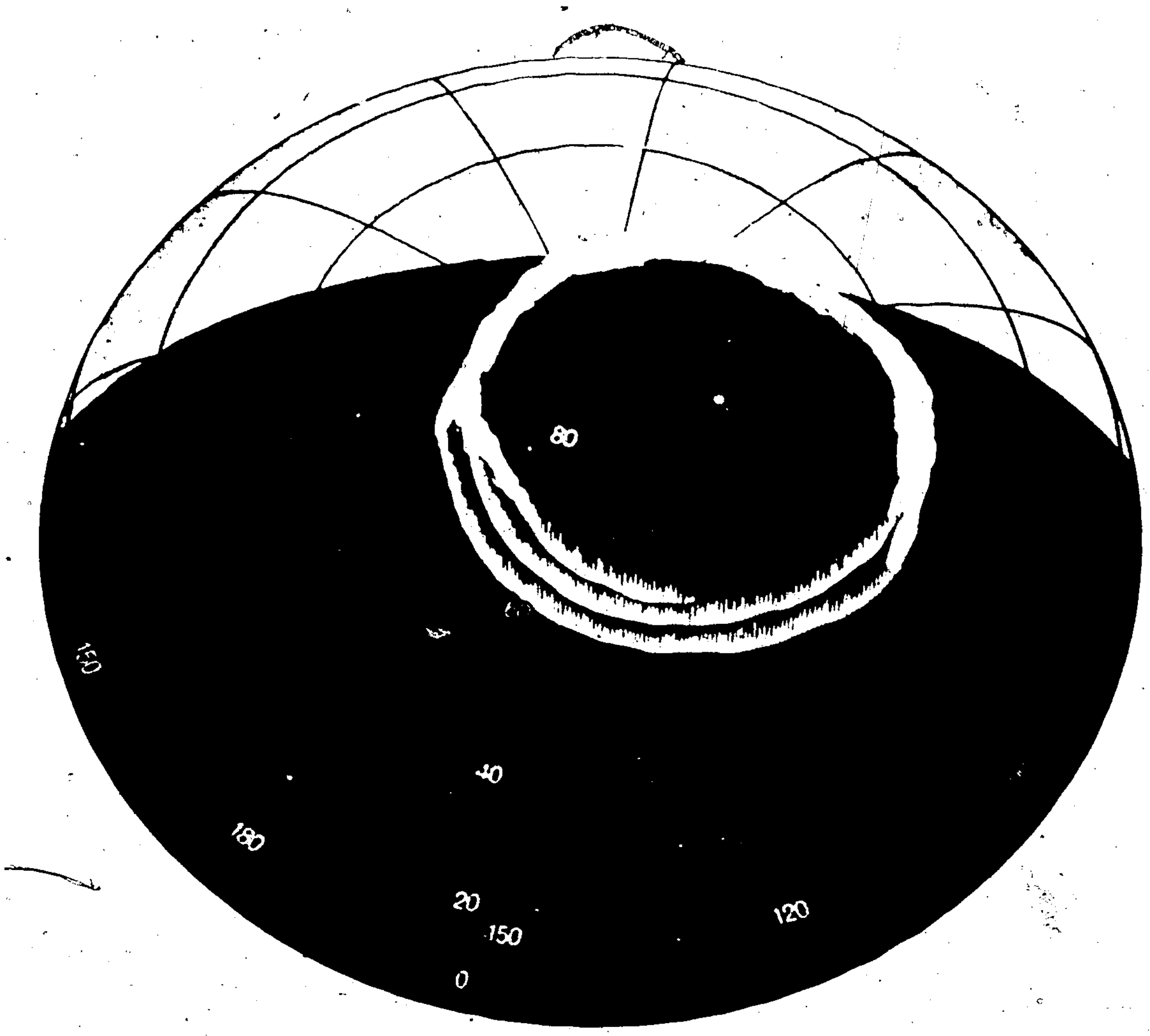

Figure 1.2

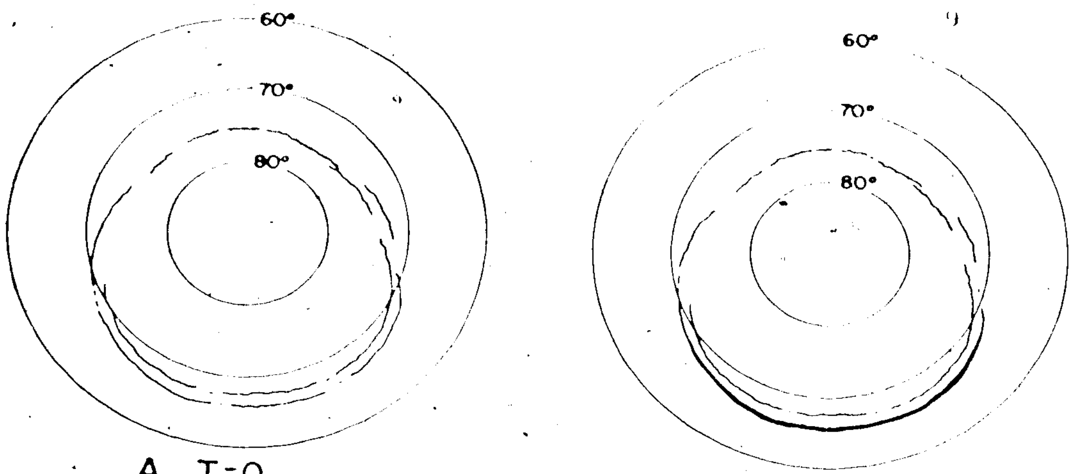

A. T=0

B. T = 0~5 MIN

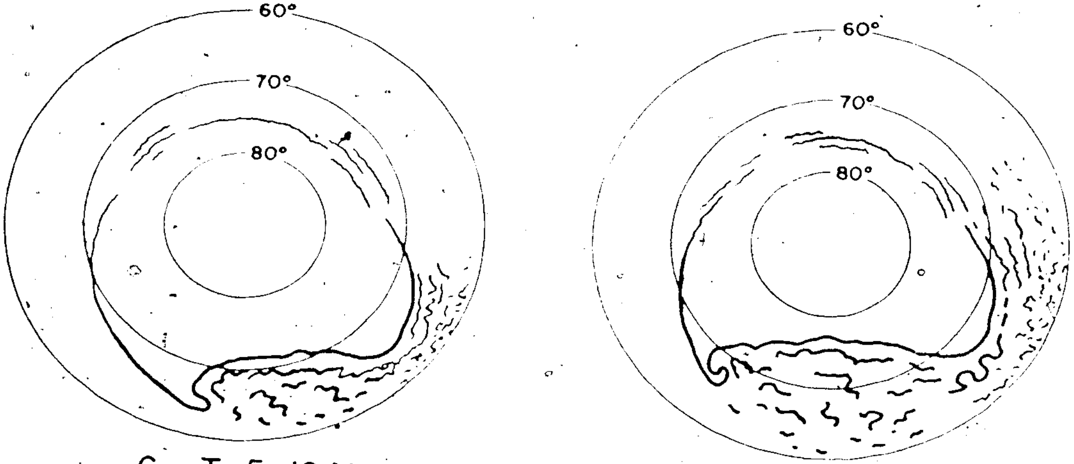

C. T=5-10 MIN

D. T=10-30 MIN

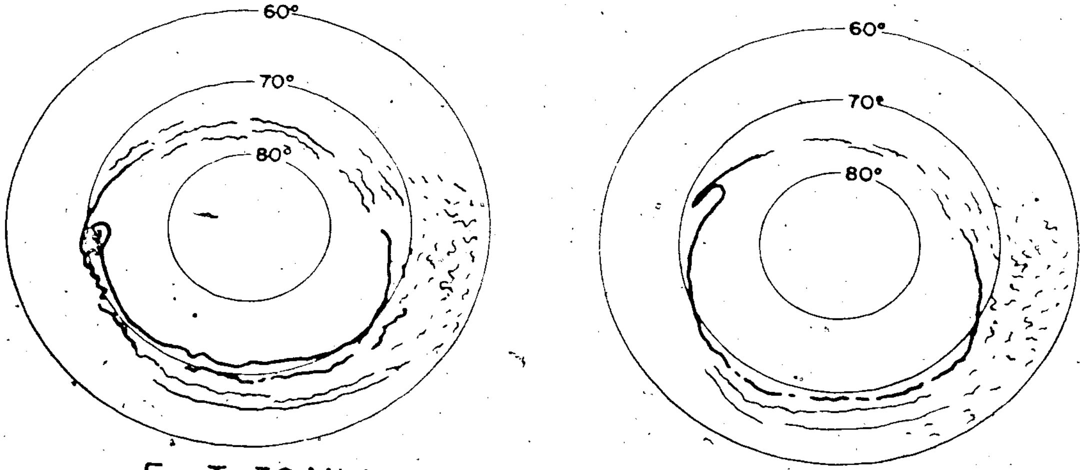

E. T=30 MIN-1 HR

F. T=1-2 HR

Figure 1.3

or the sudden formation of a new arc (B, t=0-5 min). In most cases the brightening of an arc or the formation of an arc is followed by its rapid poleward motion, resulting in an auroral bulge around the midnight sector (C, t=5-10 min). A sharp onset of a negative change in the horizontal component of the earth's magnetic field (the so-called "negative bay") is observed in the region where the brightened arc is located and also in the region swept out by its poleward motion, (namely in the bulge). As the auroral substorm progresses the bulge expands in all directions (D, t=10-30 min) and the region in which the negative bay is observed expands concurrently. The activation of the auroras associated with the poleward explosive motion spreads rapidly from the midnight sector to the morning sector, at velocities of some tens of km/sec.

In the evening sector, both the auroral and polar magnetic substorms are far more complicated than those in the morning sector. On the evening side of the expanding bulge there appears a large scale fold which travels rapidly westward along the pre-existing arcs. This particular phenomenon is called the <u>westward travelling surge</u>. When the bulge is expanding, the surge is considered to be the westward leading edge of the bulge. Thus the fact that the surge travels westward indicates westward expansion [illegible] negative bay is observed.

When the expansive bulge attains its highest latitude, the recovery phase of the substorm begins (E, t [illegible] 30-60 min). The expanding bulge begins to contract. The westward travelling surge may travel a considerable distance after the end of the expansive phase but it eventually degenerates into irregular bands. The aforementioned model has been developed by Akasofu (1964) and has remained unchanged over the years. We shall be discussing certain aspects of this model in this thesis, and we shall point out areas where some of the concepts need refining.

1.4 Polar Magnetic Substorms

The magnetogram for a typical polar magnetic substorm is shown in Figure 1.4. The magnetic disturbances are measured in the local magnetic (H,D,Z) co-ordinate system where H is the horizontal component of the main geomagnetic field measured in the local magnetic meridian plane. H is defined as positive northward, D as positive eastward and Z as positive downward in this co-ordinate system.

Polar magnetic substorms constitute the major part of the magnetic field perturbations associated with

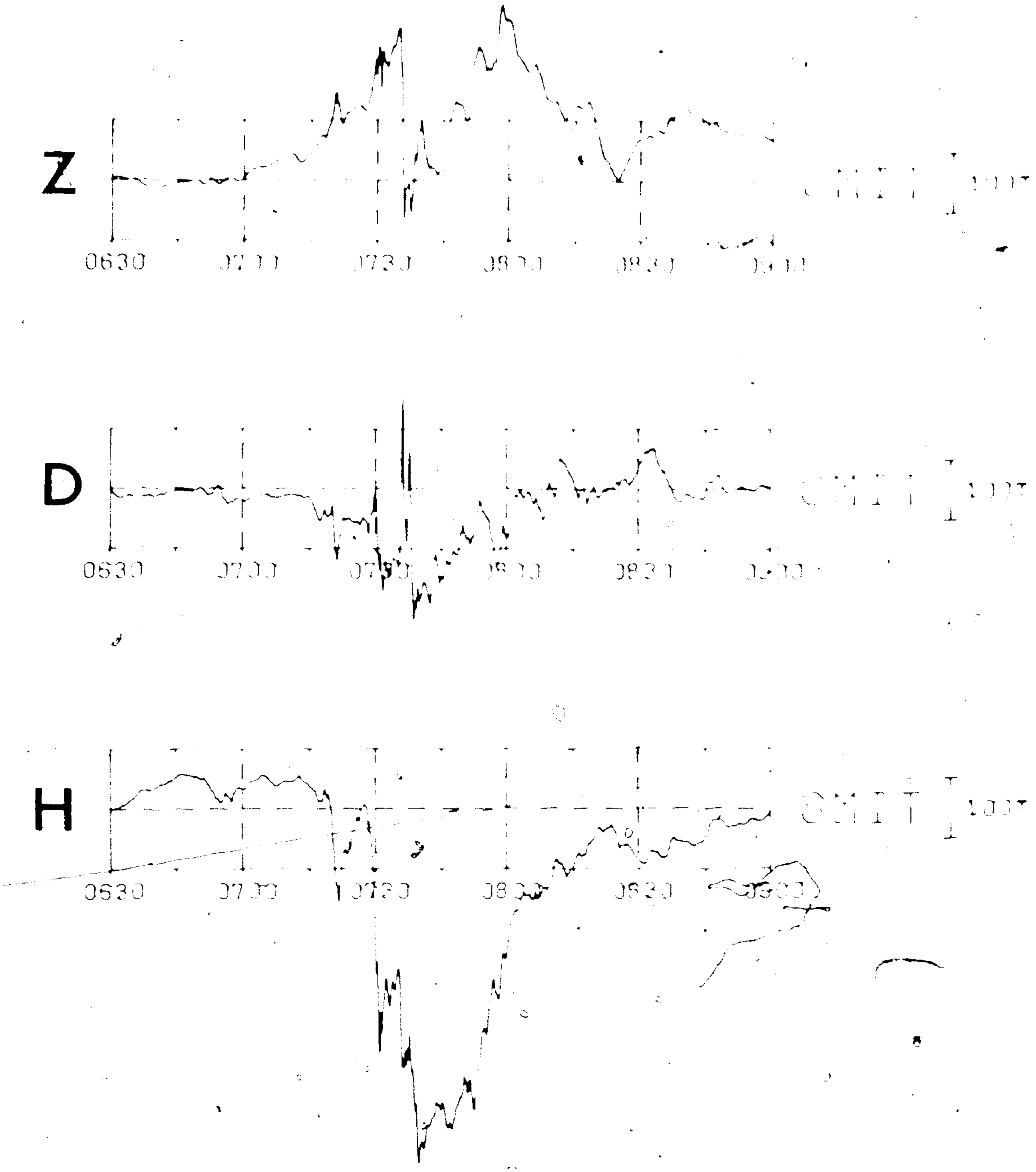
Z
0630
0700
0730
0800
0830
0900
GMT
100γ
D
0630
0700
0730
0800
0830
0900
GMT
100γ
H
0630
0700
0730
0800
0830
0900
GMT
100γ

Figure 1.3

magnetospheric substorms. They appear as large amplitude (hundreds of nT) perturbations from the base line in the region near the causative current system. The perturbations are quite sharp in the auroral oval near particularly the region of the westward travelling surge.

As discussed in the previous section, the polar magnetic and auroral substorm are closely related. Thus the general morphology of the polar magnetic substorm is similar to that of the auroral substorm. The development of the polar magnetic substorm can be broken down into at least two basic phases. The expansive phase features the sudden onset of an intense current system and the recovery phase features the gradual decay of the substorm current system over the following one to two hours.

During quiet times there exist two steady state current systems on the night-side of the earth in the auroral oval. One of these currents, called the eastward electrojet, flows in the eastward direction on the evening side of the auroral oval while the other current called the westward electrojet flows in the westward direction on the morning side of the auroral oval. The configuration of these electrojets is shown in Figure 1.5. During the expansive phase of the polar magnetic substorm, the westward electrojet expands westward into the evening sector.

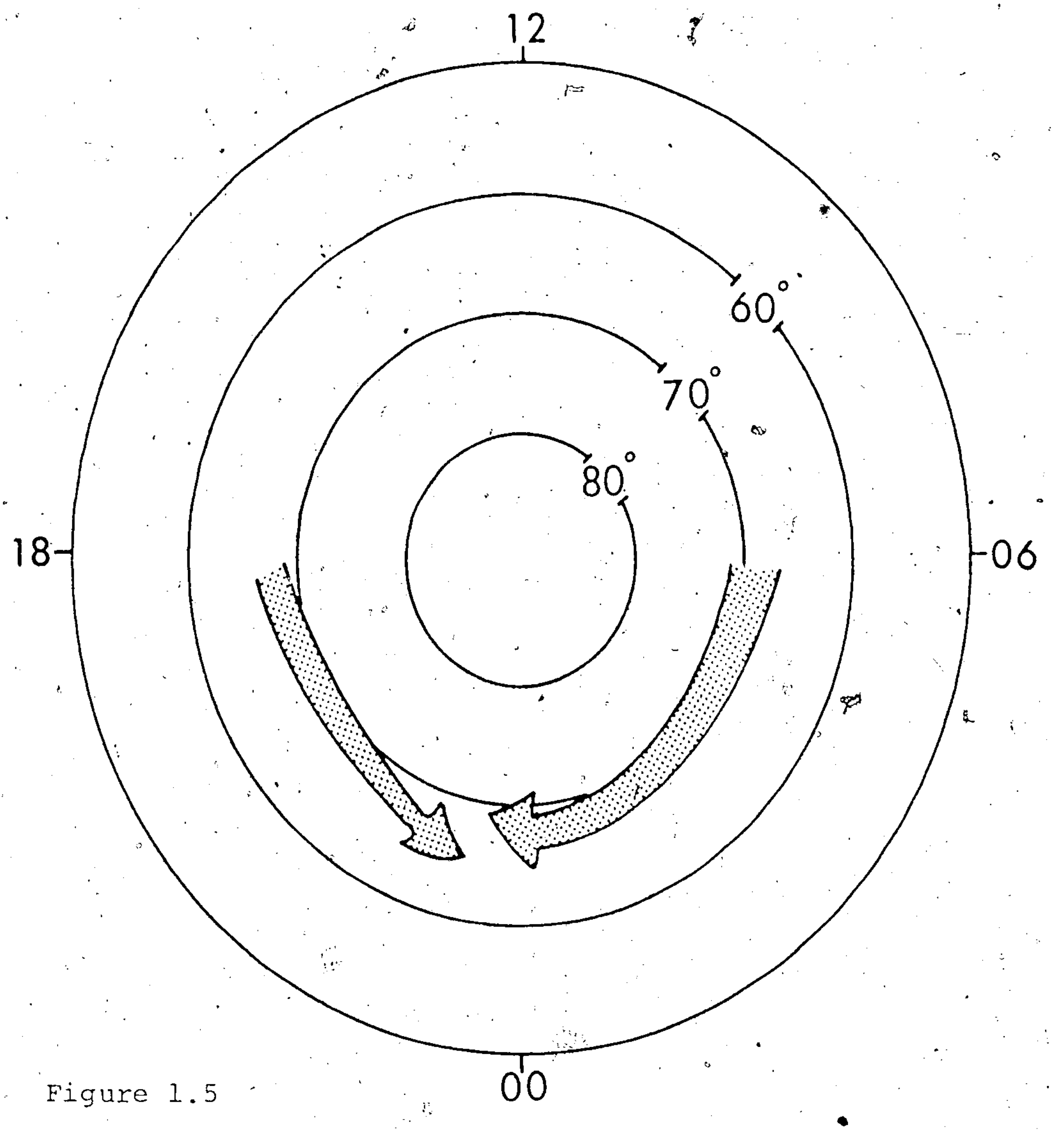

Figure 1.5

As shown in Figure 1.6, the westward electrojet expands into the region north of the pre-existing eastward electrojet. (The leading edge of the westward electrojet is associated with the westward travelling surge.) It is the region into which the westward electrojet expands where the intense negative bays are observed.

The magnetic perturbations resulting from the expanded westward electrojet have been successfully modelled (Kisabeth, 1972) by the type of three-dimensional equivalent current system shown in Figure 1.7. In this system the current flows down along the magnetic field lines to the ionosphere westward through the ionosphere and back up the field lines and closes in the equatorial plane. This current system is known as Birkeland current loop since it was Birkeland (1908, 1913) who first proposed such a current system to explain the magnetic perturbations associated with the polar magnetic substorm.

1.5 Theory of a Substorm

During the last few years a considerable number of magnetospheric and ground observations have become available, offering the possibility of a better understanding of the basic processes involved in magnetospheric and polar substorms. Many of these observations are still rather confusing and sometimes appear to conflict with one

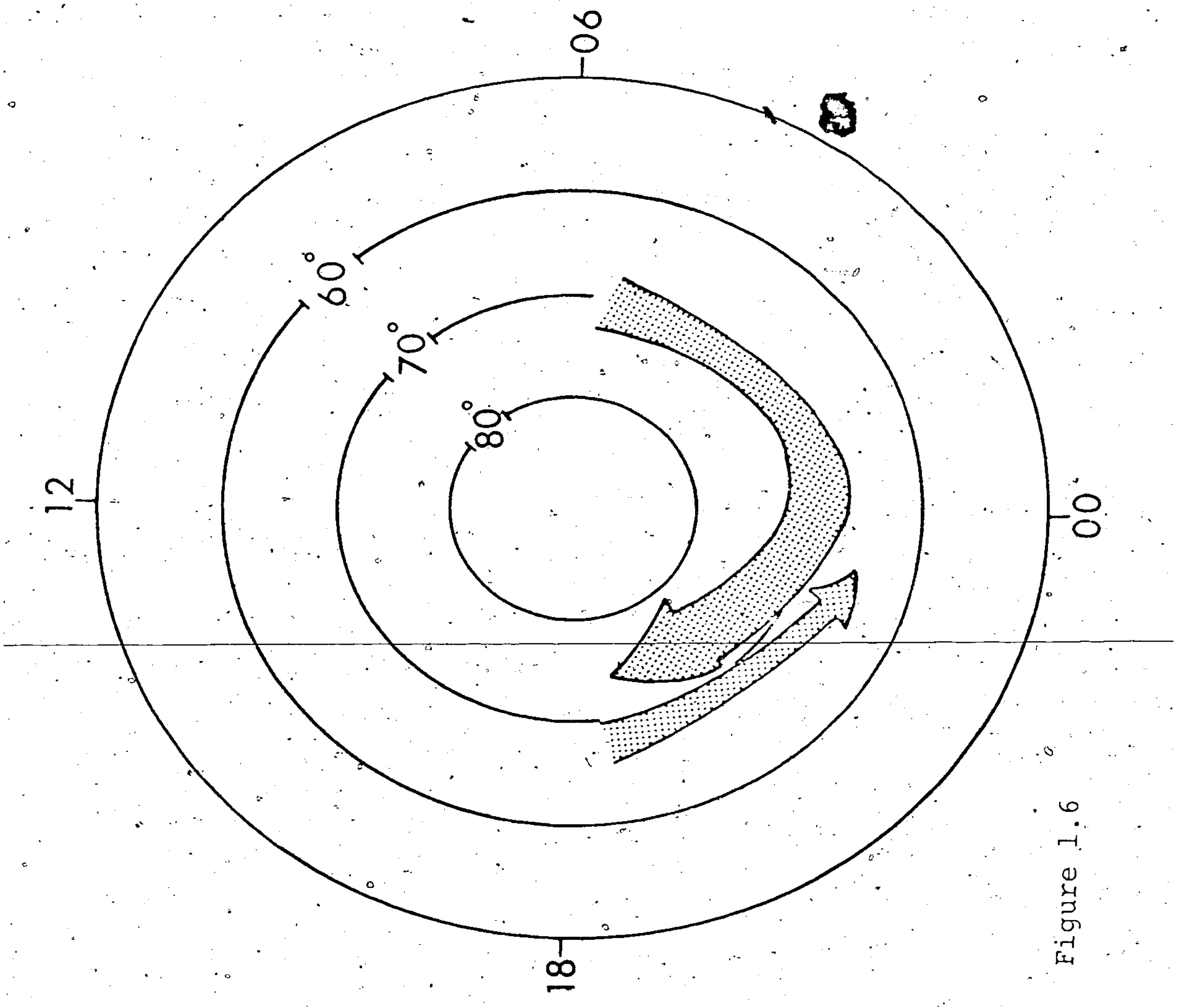

Figure 1.6

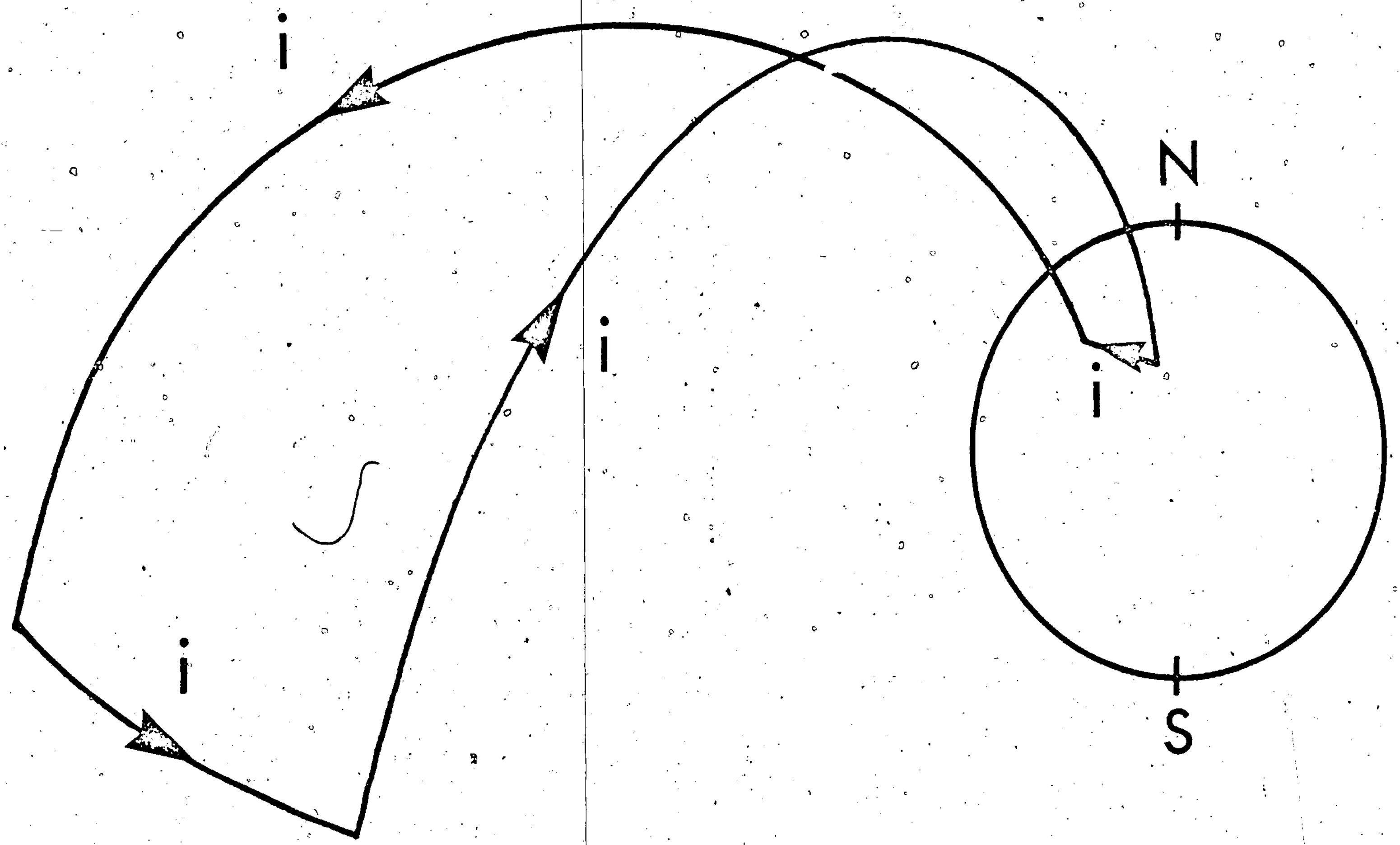

Figure 1.7

another. However a rough picture of the physics of magnetospheric substorms has begun to emerge.

Although Birkeland (1913) proposed that auroral activity was generated by streams of particles from the sun, it was Chapman and Ferraro (1931) who first realized that direct entry of the solar plasma into the nighttime auroral zone was impossible. They correctly described the interaction of the solar wind with the front of the magnetosphere, however they overlooked the presence of the interplanetary electric field and the fact that the solar wind was continuous. The original picture of Chapman and Ferraro suggested that the interplanetary space was virtually a vacuum except for times when solar flares caused streams of particles to be ejected from the sun. This misconception was corrected by Biermann (1957) who inferred from his study of comet tails that the sun was continually emitting particles, in which case the magnetosphere would be under continual dynamic pressure from the solar wind. Thus the problem becomes the definition of the means by which energy impinging on the frontside of the magnetosphere gets transferred to the night side where it may drive magnetic substorms.

1.5.1 The reconnection model

The interplanetary magnetic field seems to play a major role in the initiation of substorms and auroral activity. Many substorms occur less than one hour after the time of the turning of the interplanetary field vector component normal to the ecliptic plane from northward to southward. This correlation between the interplanetary field and substorm activity has led to the development of a reconnection model as first suggested by Dungey (1953, 1961) for substorms. The magnetosphere may be regarded as an obstacle in the path of the supersonic solar wind. When the solar wind plasma passes through the bow shock the magnetic field carried by the plasma is strengthened while its direction is changed only through a moderate angle. In Figure 1.8 the field behind the shock is taken to have a generally southward direction when the IMF is directed southward in the interplanetary medium. In this case the interplanetary field moves up to the dayside boundary of the magnetosphere and merges or connects with the field lines of the magnetosphere as shown in Figure 1.9. The newly reconnected field lines are then dragged back in the anti-solar direction by the solar wind as shown in Figure 1.8. The vital consequence of the connection of the IMF to the main field of the earth is the existence

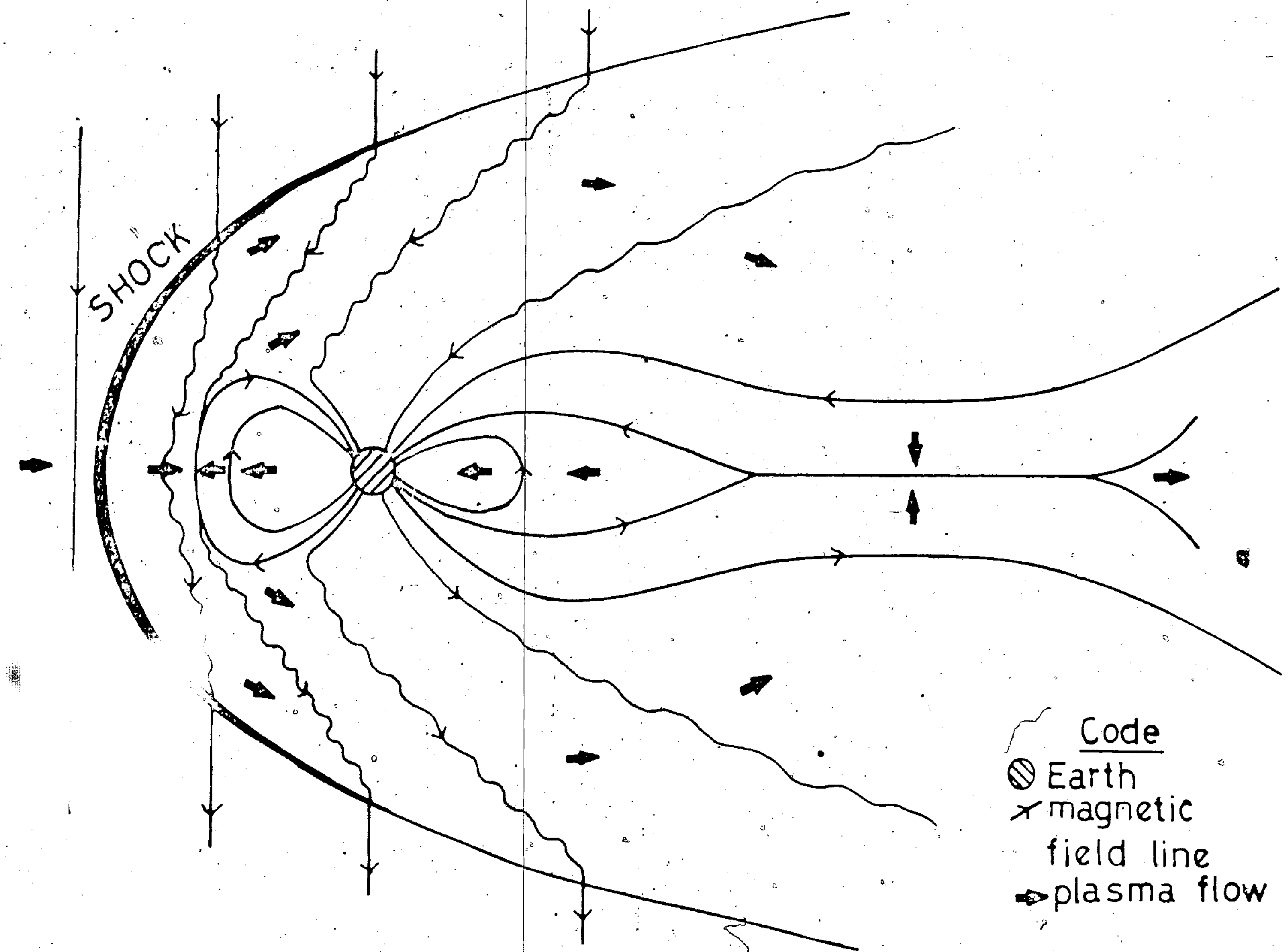

Figure 1.8

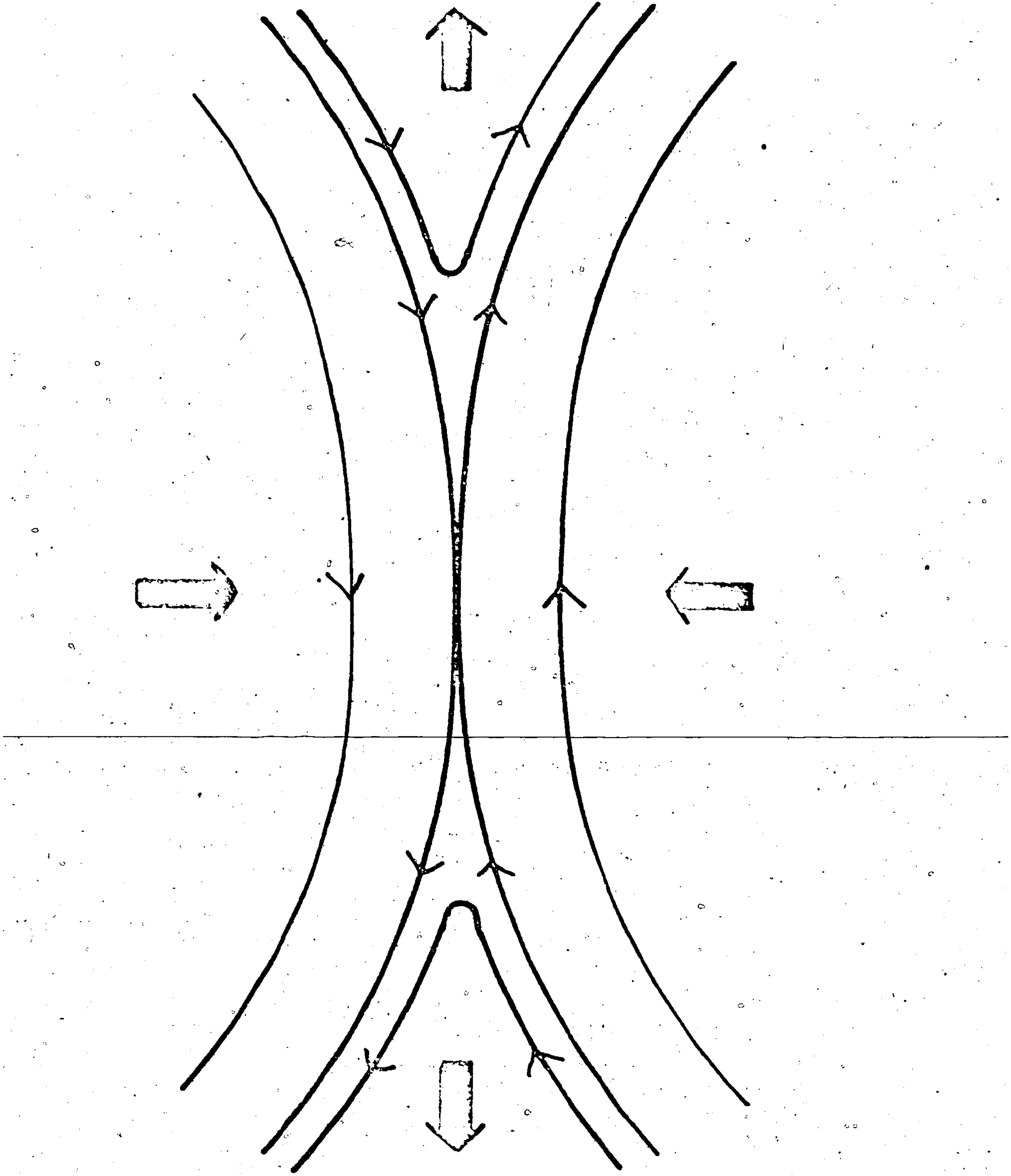

Figure 1.9

of field lines which intersect the earth through the polar caps and yet go right out into interplanetary space where they must be connected to the interplanetary field. This behaviour immediately leads to the formation of the geomagnetic tail. The part of a reconnected line which is outside the bow shock still moves with the solar wind, because outside the shock the presence of the earth is not felt. Consequently the magnetic field is stretched between a point on the polar cap and a point on the shock, which may be hundreds of earth radii downstream. Then the field in the tail is increased because all the magnetic lines of force tend to line up with the direction of the solar wind bulk flow as shown in Figure 1.8.

The tail's plasma sheet maps down into the auroral oval as shown in Figure 1.10 (Frank et al., 1971). Since reconnection on the dayside magnetosphere takes away a frontside dipole field line to form a tail field penetrating each polar cap, dayside reconnection increases the tail flux. It may therefore be expected that reconnection in the tail across the neutral sheet reduces the tail flux as shown in Figure 1.8. Petschek (1964) has shown that as reconnection takes place in the tail energy associated with the magnetic field is converted into kinetic energy of the plasma within the tail. It was

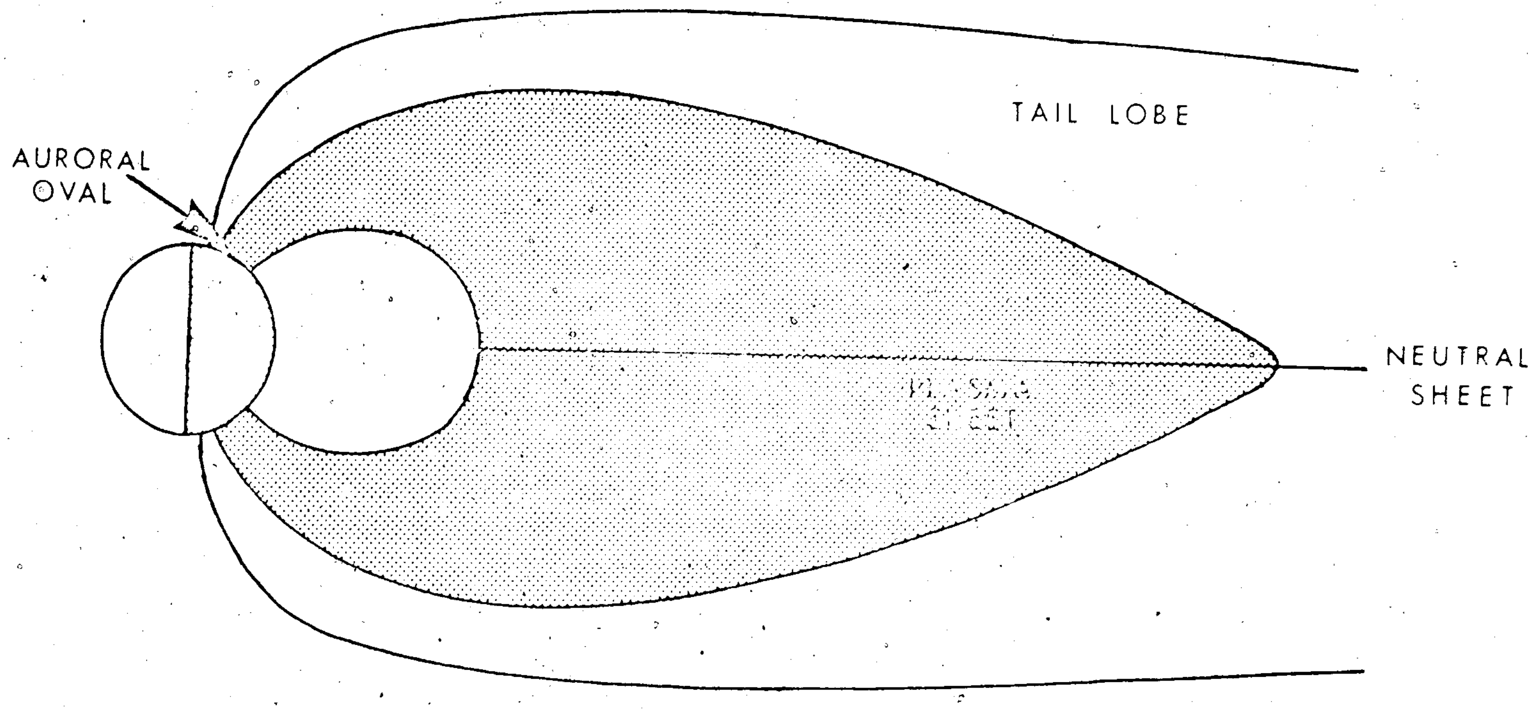

Figure 1.10

further suggested by Atkinson (1966) that while connection of the earth's magnetic field to the interplanetary magnetic field on the dayside magnetopause was a relatively continuou process, reconnection across the neutral sheet on the night side occurred in spordic bursts, each burst constituting a substorm. Then the magnetotail plasma energized during each burst of reconnection would represent the high energy particles observed in the auroral oval during a substorm.

Thus the gross picture for a substorm is one in which short lived changes in the magnetotail possibly resulting from field line reconnection, produce energetic particles that travel to the earth along lines of force which penetrate the midnight part of the oval. The particles precipitate into the ionosphere, where they produce increased Hall and Pederson conductivities. The magnetospheric changes also involve electric fields that, mapped along the magnetic lines of force, help to drive the substorm westward electrojet in the region of the ionosphere where the conductivity is increased.

1.6 Motions of the Magnetospheric Plasma

In the magnetotail within the plasma sheet there exists an electric field a major component of which is directed from dawn to dusk. Piddington (1960, 1962) and

Axford and Hines (1961) proposed that this electric field was the result of a friction or viscous-like interaction between the solar wind and the magnetosphere. This magnetotail electric field produces convective movements of the magnetospheric plasma in the equatorial plane as shown in Figure 1.11(a). However, the pattern of convection of plasma within the magnetosphere is not as simple as shown in Figure 1.11(a) as a consequence of the earth's rotation. This rotation causes the near earth geomagnetic field and its plasma to be co-rotated with the earth. When this rotational motion of the plasma is added to the convective motion shown in Figure 1.11(a) the resulting motion in the equatorial plane of magnetosphere is as shown in Figure 1.11(b).

The plasma in the region between the plasmapause and the inner edge of the plasma sheet, in addition to experiencing convective motion, undergoes drift motions which arise from the gradients in the particle density and magnetic field. The drift motions of the electrons and protons produce a current called the ring current. This ring current is centered in the equatorial plane at 4 to 6 R_E and forms a ring around the earth. During a substorm the ring current intensifies asymmetrically (Cahill, 1966). The result of this intensification is seen as a negative

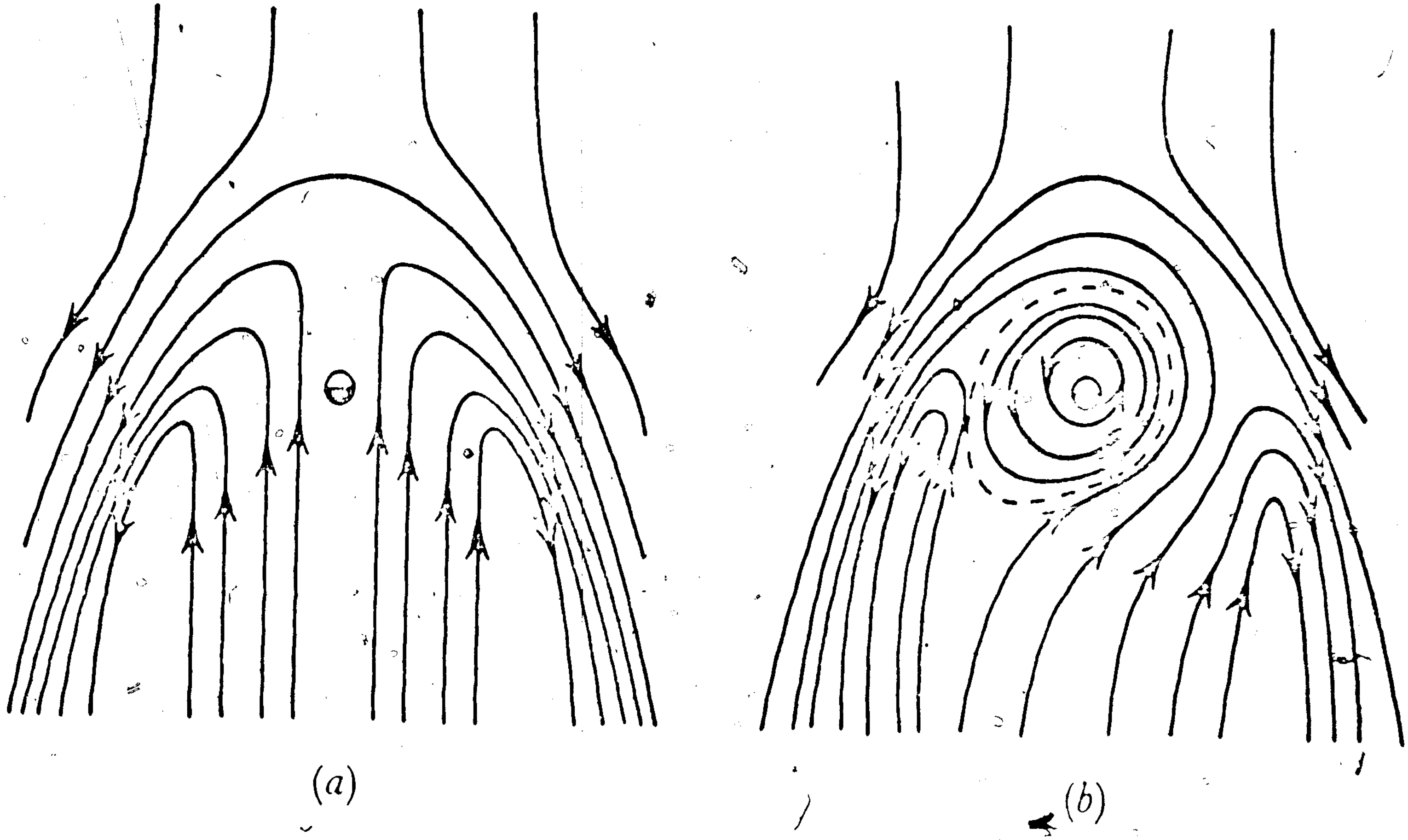

(a) (b)

Figure 1.11

perturbation in the horizontal (H) component of the earth's magnetic field at low latitudes on the earth.

Pressure gradients in the tail lead to the development of a tail current as shown in Figure 1.12 (Dessler et al., 1965). It has been suggested by Akasofu (1972) that, during a substorm, there is a sudden increase in the cross-tail electric field which leads to a sudden onset of an intense earthward ($\underline{E}\times\underline{B}$) motion of plasma in the magnetotail. It is implied that the intense motion of plasma leads to a sudden disruption of the cross-tail current causing it to flow down field lines toward the midnight part of the auroral oval from the magnetotail and back to the magnetotail from the evening part of the oval after flowing westward along the midnight part of the oval. The situation is shown in Figure 1.13. The ionospheric portion of the current system shown in Figure 1.13 would correspond to the substorm westward electrojet.

1.7 Purpose of the Thesis

Previous models accounting for the morphology of the magnetospheric substorm (Akasofu, 1964, 1968; Akasofu et al., 1966) have claimed that the westward travelling surge moves westward in a continuous manner. Since during the expansive phase the westward travelling surge has been identified as the leading edge of the westward expanding

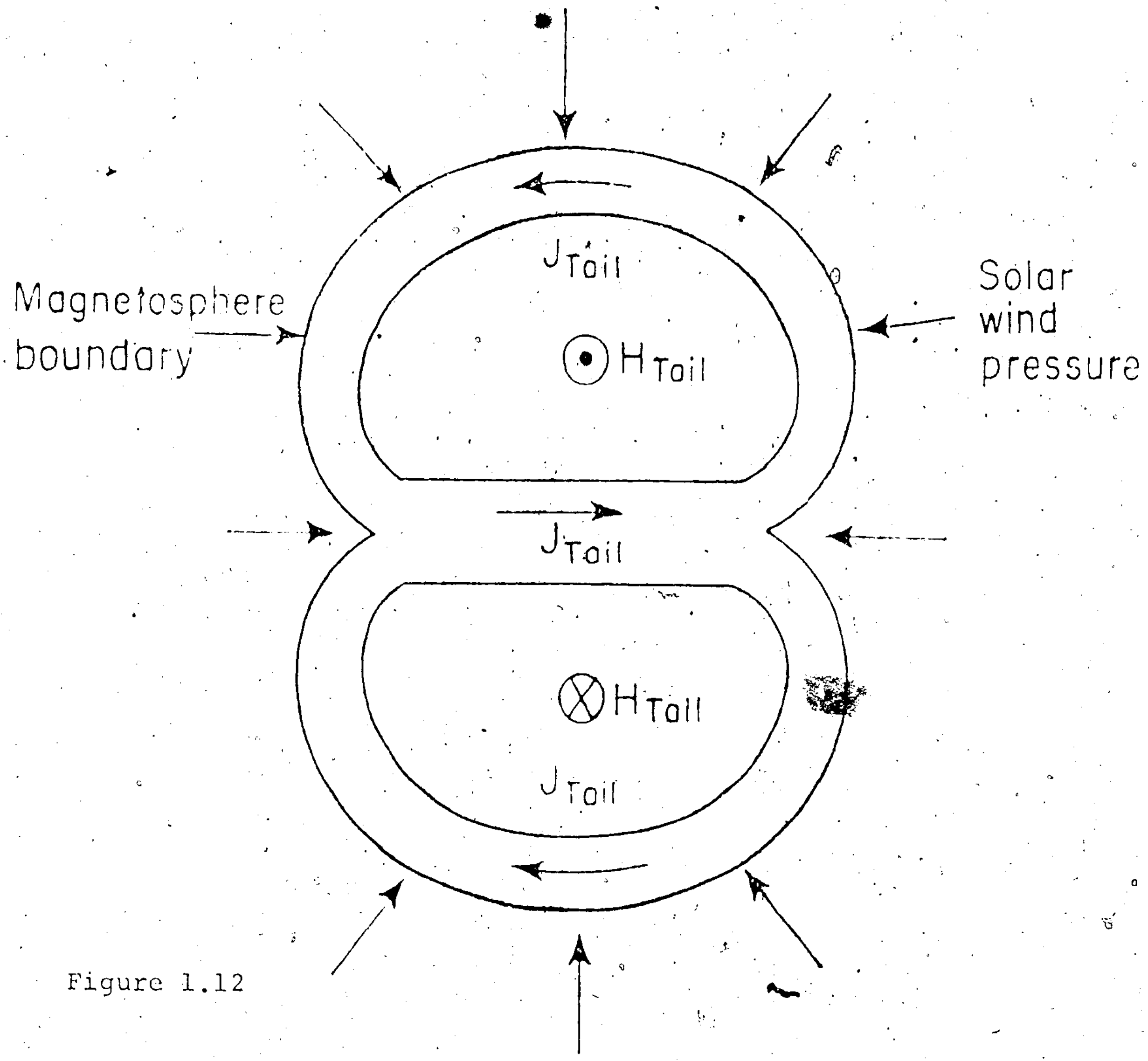
Magnetosphere boundary
Solar wind pressure
J'_{Tail}
H_{Tail}
J_{Tail}
H_{Tail}
J_{Tail}

Figure 1.12

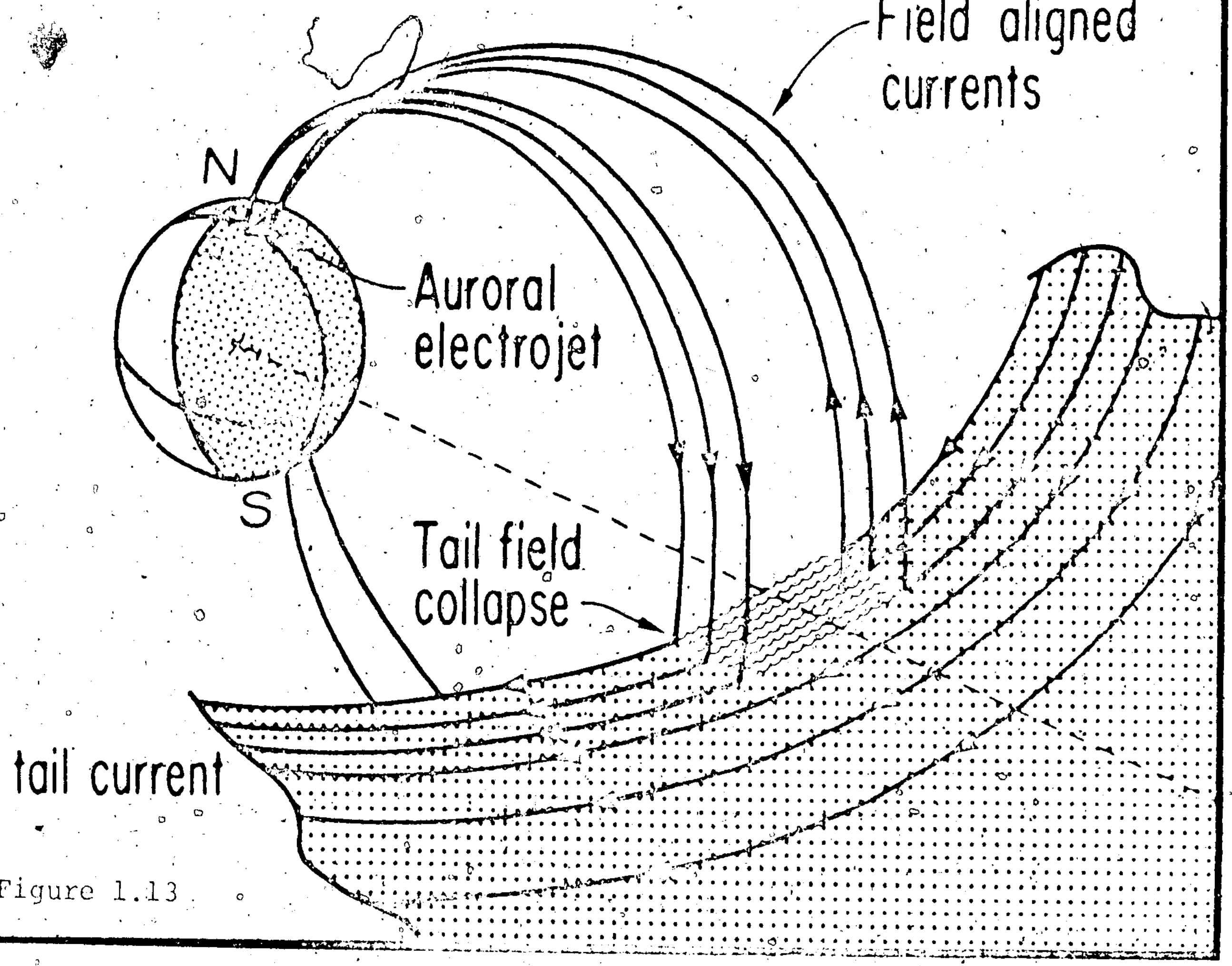
Field aligned
currents
N
Auroral
electrojet
S
Tail field
collapse
tail current

Figure 1.13

region in which intense negative bays are observed, this implies that the westward expansion of the substorm westward electrojet and the associated region of intense negative H bays is also continuous in nature.

Several recent studies using ground based magnetograms (Wiens and Rostoker, 1973; Sergeev, 1973; Vorobiev and Rezhenov, 1973; Clauer and McPherron, 1974; Kisabeth and Rostoker, 1974; Wiens and Rostoker, 1975) and satellite observations in the geomagnetic tail (Rostoker and Camidge, 1971; Hones et al., 1973) have suggested that the above picture of the polar-magnetic substorm is not an exact description of typical substorm disturbances. These authors found that there was a tendency for the substorm disturbed regions to expand northward and westw[illegible] through a series of discrete steps or jumps.

In this thesis, using an analysis of ground based magnetograms, detailed evidence will be presented for the step-wise nature of the westward propagation of the substorm electrojet.

In recent years the existence of a pre-expansive phase, termed the growth phase, has been suggested. A variety of possibilities for the ground based signature of the growth phase have been put forth by several researchers (Belyakova et al., 1968; McPherron, 1970; Kokubun, 1971; Iijima and Nagata, 1972). The observations from which these possibilities stem all seem to have at least one feature in common, namely that the ground-based observations which have been identified as indicative of growth have been so identified principally because of an expansive phase signature which shortly followed the reported observations. Thus, the ideas put forth so far have the inherent assumption that the growth phase is a unique entity and that no other substorm phase goes on at the same time as the growth phase. This assumption will be discussed in more detail based on the results presented in this thesis.

Throughout this thesis we shall use the depression of the H component of the magnetic field at low latitudes as the signature which we attribute to growth, in keeping with the suggestions of McPherron (1972, 1974) and Iijima and Nagata (1972). Therefore, when we refer to growth in the text of this thesis, we shall be referring to this particular magnetic signature. We wish to point out at this time that our use of the term growth does not imply that the physics of the process is understood. The depression in the H component may very well stem from an enhancement of the partial ring current (Fukushima and

Kamide, 1973) or from the development of upward field aligned current flow to the east of the point of observation. However, it has been pointed out by Kisabeth and Rostoker (1974) and by Rostoker (1974) that the signature of the depression in the mid-latitude H component may occur with no significant substorm activity in progress, so that we feel that we may use the term growth to be synonymous with that signature.

CHAPTER II

DATA PROCESSING AND ANALYSIS

2.1 Data Sources

To study the westward propagation of the polar magnetic substorm the magnetic observations from 36 observatories spread over the western hemisphere were used. Table 2.1 gives a list of the observatories used in this study, along with their geomagnetic (centered dipole) coordinates. Figure 2.1 is a map indicating the positions of 28 of these observatories. Some of the more southerly stations used in this study are not shown here.

Nine of the thirty-six stations (the ones marked with a star in Table 2.1) were operated in northwestern Canada by the University of Alberta. These nine observatories formed a closely spaced meridian chain arrayed along the geomagnetic meridian $\sim 300°$ E. Each of the nine stations operated by the University of Alberta recorded three components (H,D,Z) of the magnetic field variation in digital form on magnetic tape. The sample rate for the digital system was one data point for each component every two seconds, and timing was accurate to within ± 0.1 seconds. The dynamic range of the system was $\pm 1000\gamma$ with a sensitivity of $\pm 1\gamma$. The response was

TABLE 2.1

Location and Code Names of Magnetometer Stations Used in this Study

Observatory	Code Name	Geomagnetic Coordinates	
		Latitude (°N)	Longitude (°E)
Baker Lake	BAKE	73.7	315.2
Barrow	BARR	68.5	241.1
Boulder	BOUL	48.9	316.5
*Cambridge Bay	CAMB	76.8	296.6
Castle Rock	CASL	43.4	298.6
College	COLL	64.6	256.5
*Contwoyto	CONT	72.6	295.8
Dallas	DALL	42.9	327.8
Fredericksburg	FRED	49.5	349.9
*Fort Chipewyan	FTCH	66.3	302.1
Fort Churchill	CHUR	68.7	322.8
*Fort McMurray	MCMU	64.2	303.5
*Fort Reliance	RELI	70.3	300.1
*Fort Smith	SMIT	67.3	300.0
Godhavn	GODH	79.8	32.5
Great Whale River	WHAL	66.5	347.4
Guam	GUAM	3.9	212.8
Honolulu	HONL	21.0	266.4
Huancayo	HUAN	- 0.6	353.8
*Leduc	LEDU	60.6	302.9
Leirvogur	LEIR	70.2	71.0
Lerwick	LERW	62.5	88.5
*Meanook	MENK	61.9	300.8
Mould Bay	MOUL	79.0	256.3
Narssarssauq	NARS	71.0	37.0
Newport	NEWP	55.0	300.1
Ottawa	OTTA	57.0	351.5
Pamatai	PAMA	-15.3	282.8
Paramaribo	PARA	16.9	14.3
*Resolute Bay	RESO	83.0	289.4
San Juan	JUAN	29.6	3.1
Sitka	SITK	59.6	275.4
St. John's	JOHN	58.4	21.2
Thule	THUL	88.9	358.0
Tucson	TUCS	40.4	312.2
Victoria	VICT	54.1	293.0

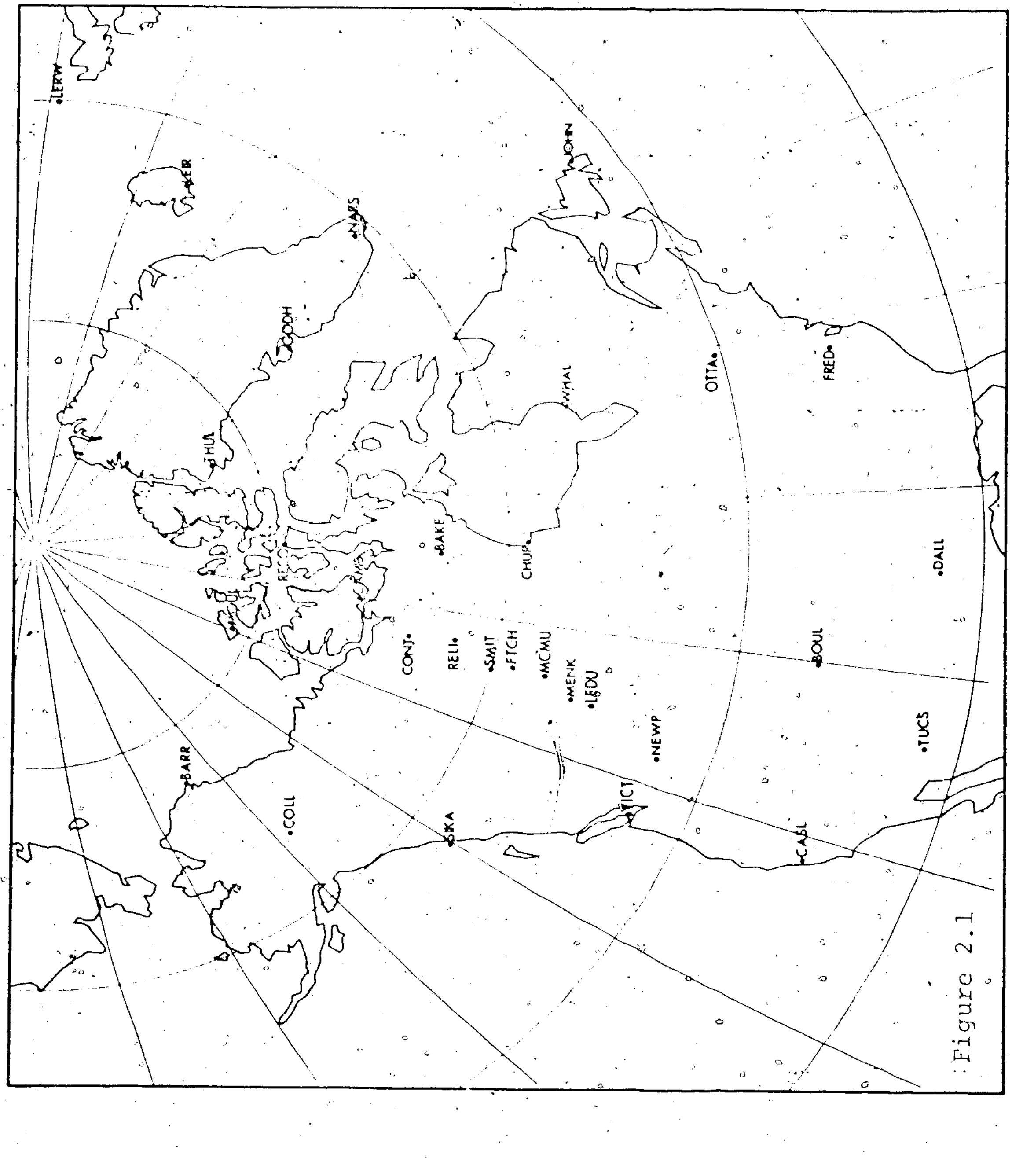
LERW
LEIR
NARS
JOHN
GODH
THUL
RESO
BAKE
CHUR
WHAL
OTTA
FRED
DALL
BOUL
TUCS
CASL
VICT
NEWP
LEDU
MENK
MCMU
FTCH
SMIT
RELI
CONJ
SKA
COLL
BARR

Figure 2.1

flat in the frequency range 0 to 0.3 Hz, with the high frequency end of the spectrum being set by the characteristics of the aliasing filters. Contwoyto Lake was manually timed and this introduced an error of about ± 30 seconds into its timing.

The magnetic records of the remaining 27 stations were recorded on a paper chart except for Castle Rock. Copies of the magnetograms for these stations in microfilm format were obtained from the World Data Center A for Solar-Terrestrial Physics. The magnetograms on microfilm were photographically enlarged and then digitized. This process introduced an error of ± 1 minute into the timing of data from these stations. Castle Rock was the only station not operated by the University of Alberta for which the data were digitally recorded. The magnetic records for Castle Rock were supplied in digital form on magnetic tape with a sample rate of one data point for each component every 2.5 minutes.

2.2 Data Format

In the study of spatial and temporal development of the substorm westward electrojet three different methods of presentation of the data from the magnetic observatories were used

2.2.1 Component magnetogram format

In this method the H, D, or Z components of the magnetic data from a selection of the 36 observatories for a specified period of time are plotted with either the northernmost or easternmost station at the top of each plot. This method of data presentation was used mainly to allow interpretation of the relation between stations to the specific event being studied.

2.2.2 Three-dimensional diagrams

A more quantitative method of presenting the data from the University of Alberta's line of stations was accomplished by generating a perspective view of the H-component as a three-dimensional surface. This was accomplished with the use of a perspective plotting subroutine written by H. Jesperson (Iowa State University) and modified by R. J. Beebe (Stanford University). Although there is a loss of information as compared with that available from component magnetograms, such 3-D plots are especially useful for showing the spatial and temporal developments of the substorm westward electrojet.

2.2.3 Polar plots

To display the magnetic data from stations distributed both in latitude and longitude the vectors representing the total horizontal component of the perturbation field for each station were plotted in centered dipole coordinates on polar plots. This method of data presentation was used because it makes use of both the H and D components to determine the position of the substorm westward electrojet. Although the distribution of available stations is rather sparse in many areas the nature of a polar plot allows one to obtain valuable information about the position of the substorm westward electrojet. This is discussed in more detail in the section below.

2.3 Study of Westward Jumping of Substorm Electrojet Activity on Day 357, 1971

Figure 2.2 shows the magnetograms for the interval 0300-0700 UT on Day 357, 1971, from the meridian chain of stations which was operated in north-western Canada by the University of Alberta. The behaviour of the H-components in this figure is typical of the pattern of substorm development observed along a meridian line. That is, the onset of a negative H bay is observed first at stations near the bottom of the chain (in this case at ~ 0436 UT at FTCH and SMIT) with the onset of a negative H bay being seen about ten minutes later at CONT and another twelve minutes later at CAMB. The sharpness of each of the

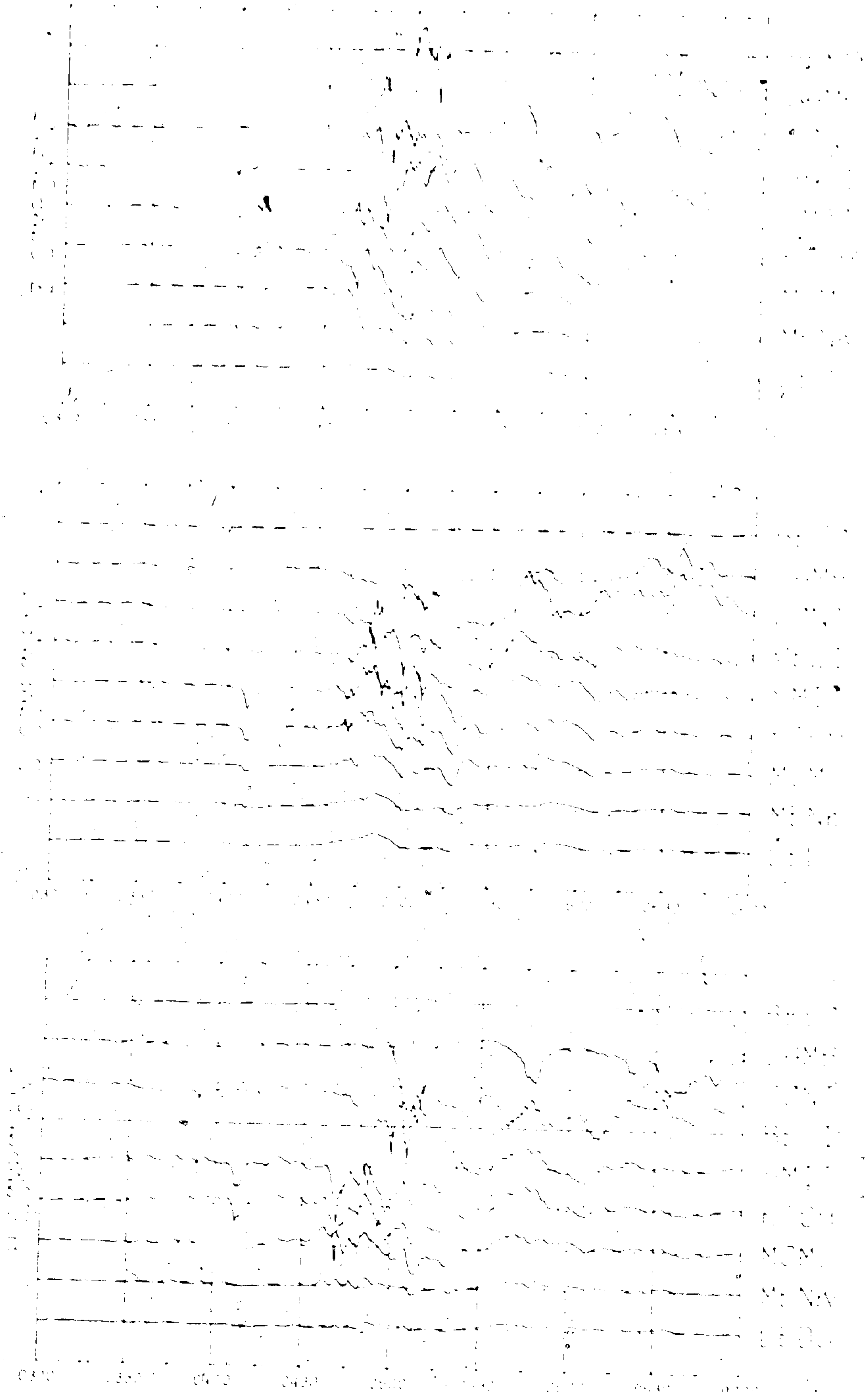

Figure 2.2

negative H bay onsets seen in Figure 2.2 suggests that the observed delay between onsets is not due to a westward electrojet which is simply expanding northwards in a continuous manner. Moreover, inflections in the Z component can be seen to occur in conjunction with each of the negative H bay onsets. A continuous expansion of the electrojet northwards cannot explain the association of a Z component inflection with a negative bay onset. Thus the sharpness of the negative H bay onsets together with the occurrence of an inflection in the Z component in conjunction with each of these negative H bay onsets suggests that the westward electrojet propagates to the [illegible] through a series of steps or jumps. A 'three-dimensional' picture of the development of the H component for this particular substorm is shown in Figure 2.3. The impulsive nature of the northward expansion of the westward electrojet is made apparent by the form of each of the three successively northward displaced 'mountain peaks'.

It was the frequent occurrence of the type of observation described above which led to this study involving a more extensive distribution of magnetic observatories in the western hemisphere designed to test the hypothesis that the westward expansion of the substorm westward electrojet was step-like rather than continuous in nature.

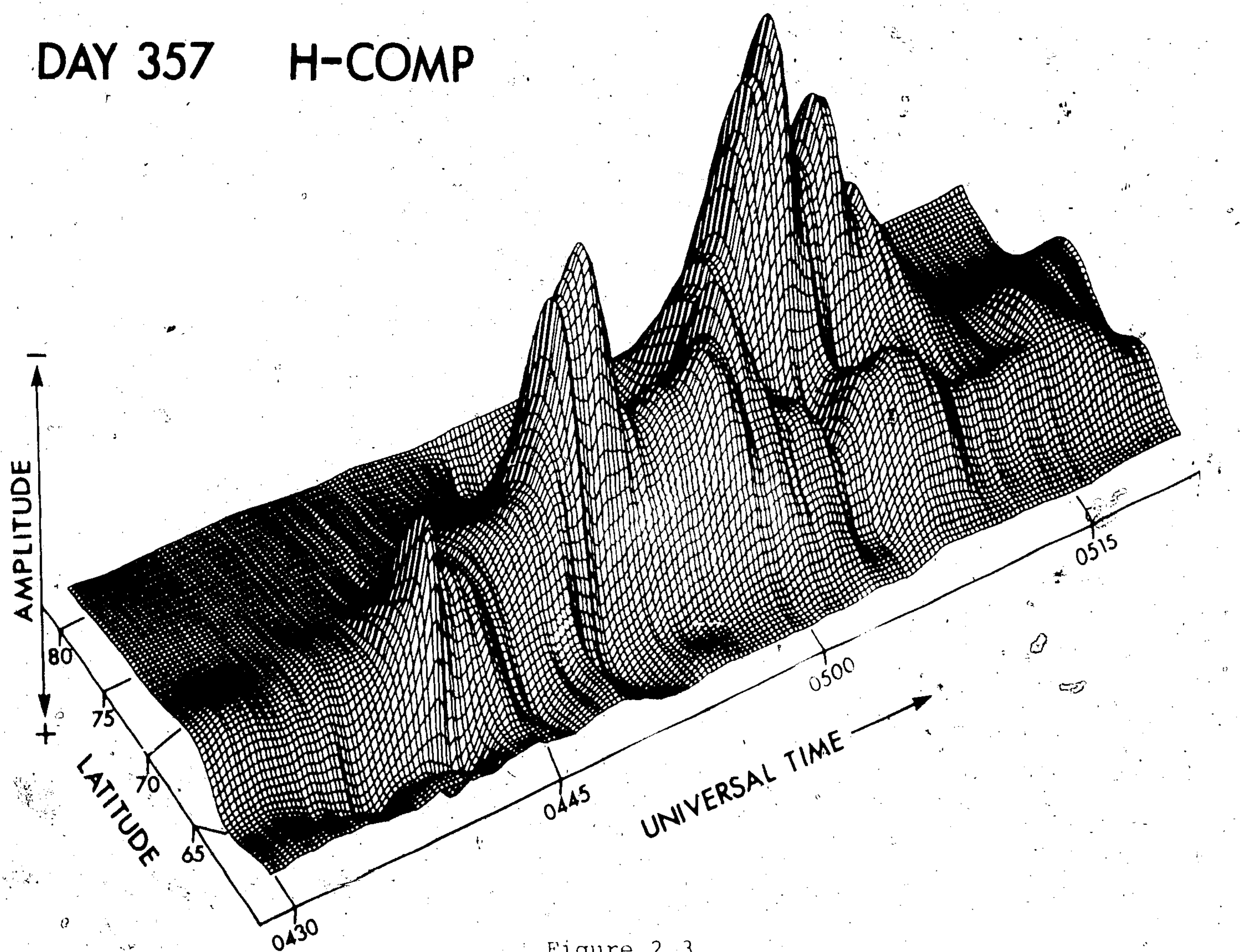
DAY 357 H-COMP
AMPLITUDE
–
+
LATITUDE
80
75
70
65
UNIVERSAL TIME
0430
0445
0500
0515

Figure 2.3

Figure 2.4 shows the H, D, and Z components for the interval 0200-0800 UT on Day 357, for other high-latitude stations to the east and west of the meridian chain of stations. From Figures 2.2 and 2.4 it can be seen that there was a substorm onset near WHAL at 0430 UT. None of the stations to the east of WHAL or west of the meridian chain showed any sharp onset of negative H bays for the period shown here. Thus substorm activity for Day 357 was confined between an area which extended from the WHAL region to just west of the meridian chain.

Figure 2.5 shows the observations of the H component for Day 357 from mid- and low-latitude stations. The stations are arranged in an east-west manner in this figure so that the most easterly station (geomagnetically speaking) is plotted at the top of the figure.

The magnetic signature at mid-latitudes of a Birkeland current loop such as that shown in Figure 1.13 is due to the integrated effects of a ring or tail current perturbations and the field-aligned currents connecting with the auroral electrojet in the ionosphere (Bonnevier et al., 1970). Figure 2.6 shows the mid-latitude magnetic signature of such a current loop as modeled by Clauer and McPherron (1974). Note that in this figure, north corresponds to the H-component while east corresponds to

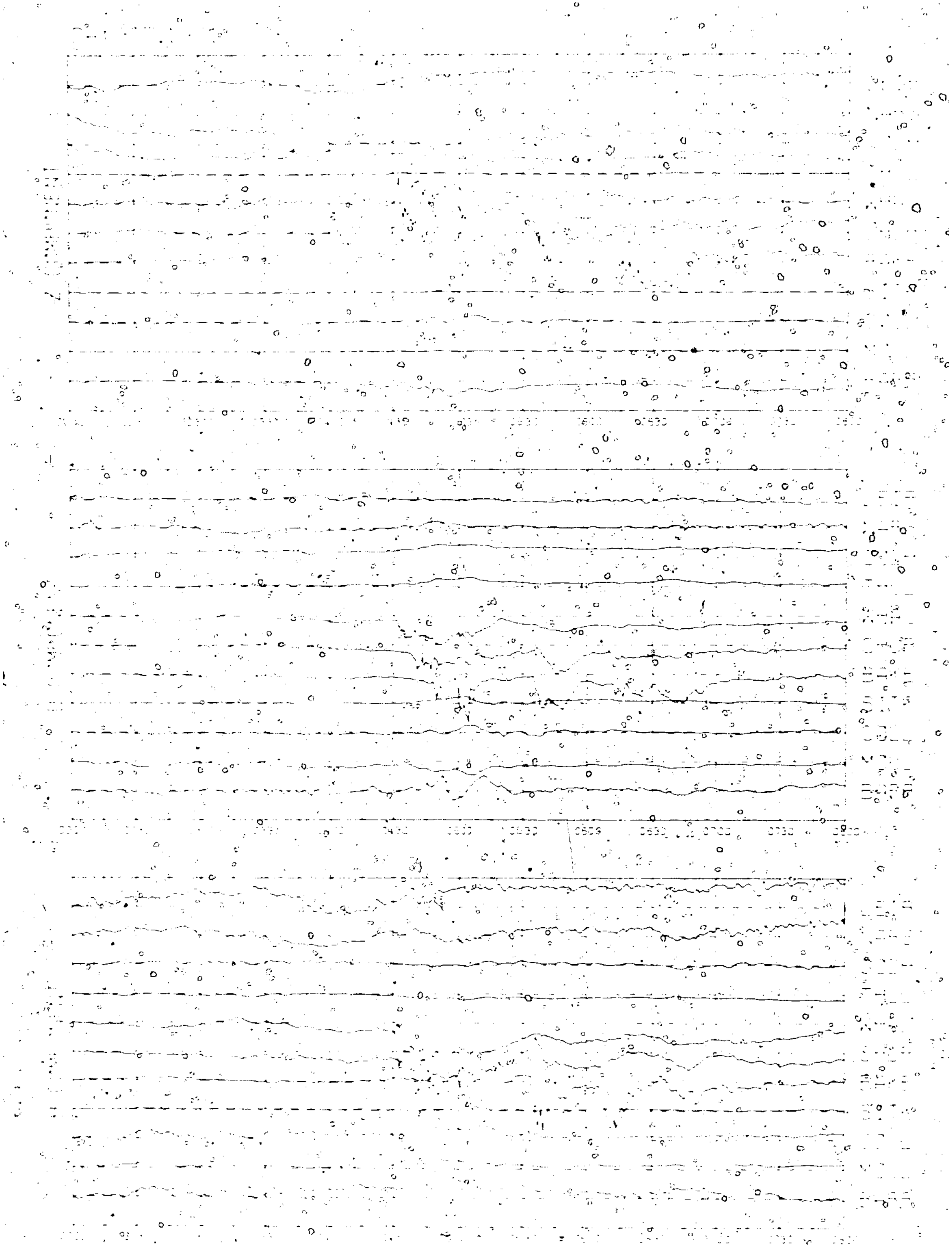

Figure 2.4

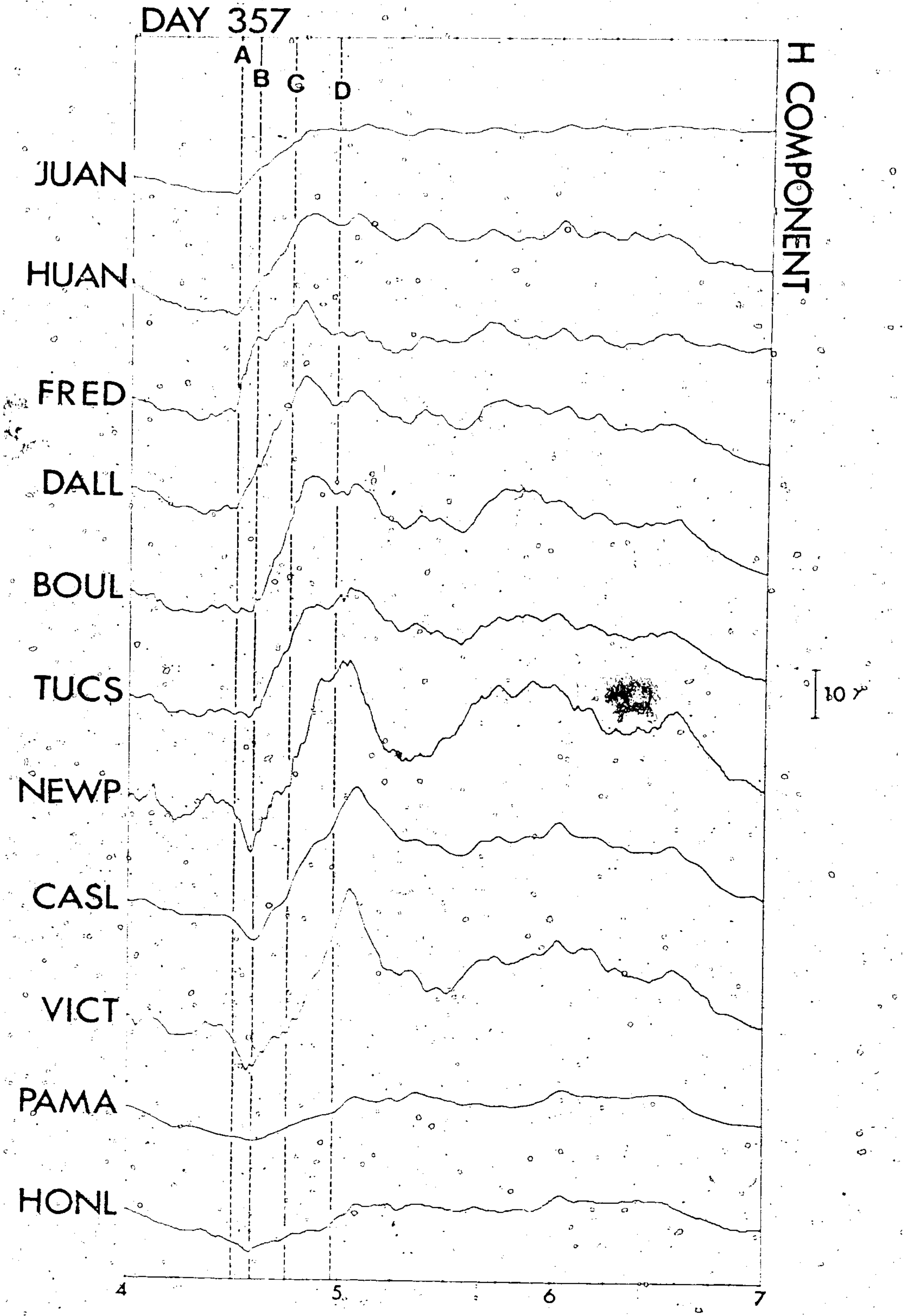
DAY 357
A
B
C
D
H COMPONENT
JUAN
HUAN
FRED
DALL
BOUL
TUCS
NEWP
CASL
VICT
PAMA
HONL
10 γ
4
5
6
7
UNIVERSAL TIME

Figure 2.5

Model of Substorm Expansion

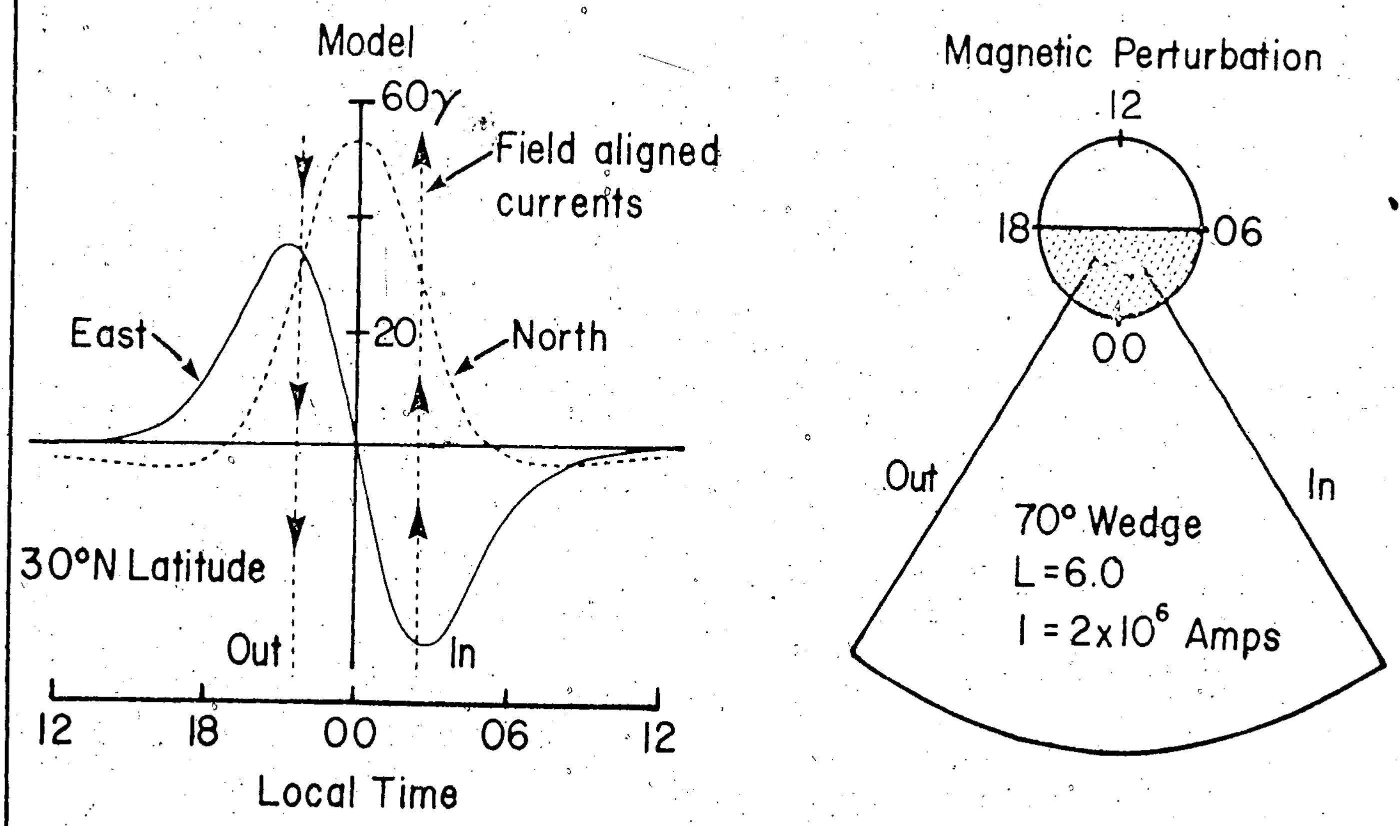

Figure 2.6

the D-component. From Figure 2.6 it can be seen that the H-component undergoes a positive change at mid-latitudes situated within the wedge defined by the field-aligned currents while mid-latitude regions to the east and west of this wedge experience a negative change in the H-component. Thus in terms of equivalent Birkeland currents, a positive change in the mid-latitude H-component can be interpreted as due to short circuiting of the ring or cross-tail current down field lines to the auroral zone (Kamide and Fukushima, 1972; Akasofu, 1972; McPherron et al., 1973). Thus a positive enhancement of the mid-latitude H-component can be associated with the onset or enhancement of a westward electrojet in the auroral oval. Thus the changes in the H-component observed at mid-latitudes can be used if adequate station coverage exists to define the longitudinal extent of the substorm westward electrojet.

Inspection of Figure 2.5 shows that at 0430 UT (event A) a mid-latitude onset of a +ΔH is observed at JUAN, HUAN, FRED and DALL while the H component at BOUL and TUCS remain relatively level. NEWP, CASL, VICT, FAMA and HONL all show an onset or enhancement of a negative H component slope at this time indicating growth in their sectors. About six minutes later at 0436 UT (event B) all stations from BOUL westward show the onset of a positive bay in the H component. JUAN, FRED and DALL which are to the east of BOUL show an inflection in their positive slope at this time.

Thus the mid- and low-latitude stations shown in Figure 2.5 indicate that there were two disturbances, one at 0430 UT and another at 0436 UT. The mid-latitude magnetograms also show that these two disturbances were not due to one simple disturbance which was just propagating westwards. If this were so, one would expect to see successive onsets of a positive H bay between adjacent stations as the disturbance progressed westwards. However, this most definitely is not what was observed. Associated with event A was the onset of a $+\Delta H$ at one whole group of mid- and low-latitude stations stretching from JUAN to DALL while for event B a second group of stations from BOUL to HONL showed a simultaneous onset of a $+\Delta H$. This observation strongly suggests that the propagation of the disturbance westwards was not a continuous motion but was more jump-like in nature.

By 0436 UT all the mid- and low-latitude stations shown in Figure 2.5 have experienced an initial onset of a positive H bay. Thus onsets of events subsequent to event B can n[illegible] determined by observation of the corresponding mid-latitude positive H bay onset. The remaining two events (C and D) shown in Figure 2.5 were not determined from the mid-latitude magnetic observations but were ascertained from onsets of intense negative H bays observed at high-latitude stations. These high-latitude observations are discussed below. It can be seen from Figure 2.5 that these last two events (C and D) correspond to intensifications in some of the already existing mid-latitude positive H bays.

Figure 2.7 shows a composite of all the high-latitude stations which experienced onsets of intense negative H bays during the period 0400 to 0700 UT on Day 357. As can be seen from Figure 2.7, WHAL experienced an onset of a negative H bay at 0430 UT. The time of the onset of the bay at WHAL corresponds exactly to the onset of event A observed in the mid-latitude magnetograms. A second onset of a magnetic expansion phase is seen about six minutes later at CHUR, SMIT and FTCH. The onset of the expansion phase at SMIT and FTCH is taken from the time of the sudden positive H component excursion just prior to the onset of a negative H bay. Such a positive enhancement can occur when the onset of a westward electrojet involves an auroral loop or surge just to the north of the station in question (Kisabeth and Rostoker, 1973). The auroral loop

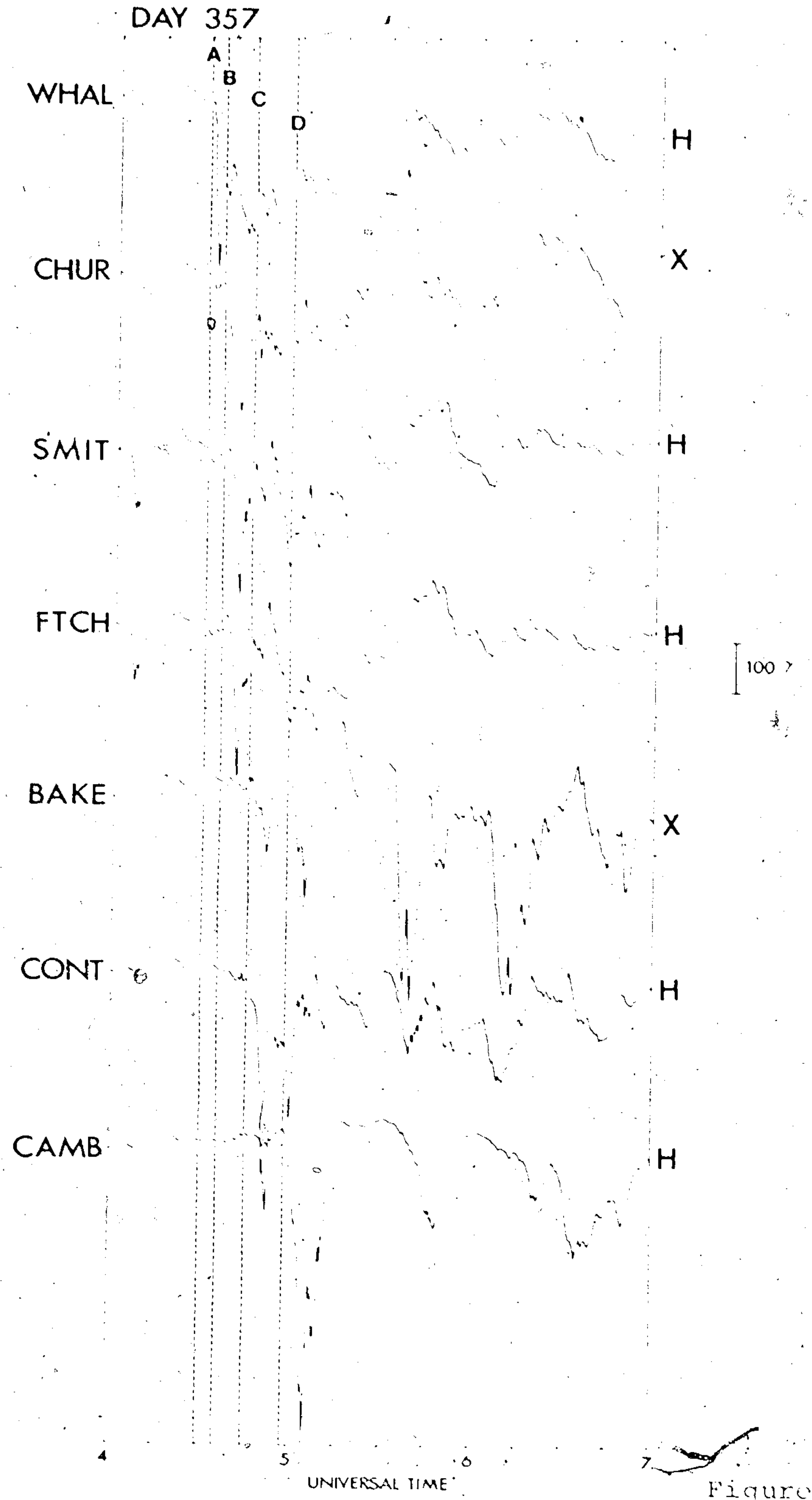
DAY 357
A
B
C
D
WHAL
H
CHUR
X
SMIT
H
FTCH
H
100 γ
BAKE
X
CONT
H
CAMB
H
4
5
6
7
UNIVERSAL TIME

Figure 2.7

or surge initially masks the onset of the substorm electrojet. Thus, in this case, the onset of a substorm electrojet probably occurred slightly north of SMIT and FTCH but in conjunction with the onset of the event B observed in the mid-latitude stations.

Thus, the high-latitude recordings, when taken in conjunction with the mid-latitude magnetograms, show that an event (A) occurred at 0430 UT and that another event (B), occurred at about 0436 UT. Event A featured the onset of an intense westward electrojet in the WHAL region while event B involved the onset of a second intense westward electrojet in the CHUR-FTCH region.

The second event observed at CHUR, FTCH and SMIT cannot be just an extension of the first event. That is, if the westward electrojet initially appears in the WHAL region, it is then not possible to interpret the second event (B) as simply the result of the electrojet located in the WHAL region either expanding or moving continuously up the auroral oval with such stations as CHUR, FTCH and SMIT showing intensifications or onsets as the electrojet expands over them. Indeed it may be tempting when looking at CHUR, which shows at 0430 UT (coincident with the WHAL onset) a gentle sloping negative H bay, to say that CHUR is seeing the effect of the westward electrojet moving towards it and that CHUR experiences an intensive negative H bay when this electrojet expanded into the CHUR region. The chief objection to the above interpretation is that the onsets at CHUR, SMIT and FTCH were coincident which seems to rule out the possibility that the onsets were due to an electrojet which was continuously expanding westwards. Therefore, the sloping negative H bay at CHUR is considered to be merely the signature of the development of the distant electrojet in the WHAL sector. Thus, the high-latitude magnetograms are in agreement with the mid- and low-latitude magnetic observations in suggesting that from event A to event B the western end of the substorm westward electrojet expanded to the northwest in a step-like fashion.

Further study of the high-latitude magnetograms shown in Figure 2.7 reveals that at 0445 UT a third onset was observed at BAKE and CONT (event C) and then at 0458 UT a fourth intense onset of a substorm westward electrojet (event D) was observed at CAMB with a simultaneous intensification of the electrojet located in the CONT-BAKE region. Looking at the mid- and low-latitude stations shown in Figure 2.5 it is seen that the onset of the BAKE-CONT event (event C) coincided with clear intensifications at CASL and NEWP while the CAMB event (event D) coincided with an intensification at PAMA.

After event D no further onsets were observed west of CAMB. The peak of the negative H bay at CAMB at 0505 UT (Figure 2.7) corresponds to the peak of the positive bay at CASL, VICT, FAMA and HONL. Thus, it is probable that after event D there was no further westward development of the substorm electrojet system; that is, no new westward electrojets developed to the north and west of CAMB. However after event D, onsets and intensifications of negative bays were observed in the region where electrojets had previously existed. Periodic intensifications of positive H were also observed in all the mid- and low-latitude stations after event D. However these intensifications never matched the [illegible] of the disturbance reached during event D. Shortly after 0630 UT both mid- and low-latitude staitons show a cessation of activity as can be seen in Figures 2.5 and 2.7.

From Figure 2.4 it can be seen that at the time of the maximum of the negative H bay at WHAL for event A the Z component at that station was in the midst of a transition going from positive to negative. This indicates that WHAL was very close to the north-south center of the substorm westward electrojet. Since the maximum magnetic perturbation resulting from a substorm westward electrojet occurs where the center of the electrojet is directly overhead, it is most likely the case that the maximum negative perturbation observed at WHAL of 330 nT represents the maximum magnetic perturbation associated with the substorm westward electrojet (event A). If a Birkeland current loop is the correct representation of the substorm current circuit, then the ratio of high-latitude to mid-latitude H-component perturbations should be of the order of 20 to 1 (Kisabeth, 1972). Comparing figures 2.5 and 2.7 it can be seen that, at the time of the maximum of the negative H bay at WBPL (330 nT), the mid-latitude station FRD experienced a positive H bay of about 10 nT. Thus the ratio of high-latitude to mid-latitude H component perturbation for event A is about 30 to 1. This ratio is a little higher than the 20 to 1 ratio expected for a Birkeland current loop. However, as Kisabeth (1972) points out, the ratio of 20 to 1 is only valid for observations taken along the central meridian of a current system (i.e. that line which divides the substorm westward electrojet into an eastern and western half) and the ratio increases as one moves off the central meridian. Thus the observed ratio is not unreasonable and the use of the Birkeland current loop as a model for the substorm current circuit would appear to be acceptable.

The central meridian of an electrojet can be used to study the westward motion of that electrojet. (The central meridian of an electrojet is defined as that line which bisect the electrojet into two parts, an eastern half and a western half). If, for example, the substorm westward electrojet is expanding continuously westwards, then the corresponding westward displacement of the central meridian should also be observed to take place in a similar continuous fashion.

The position of the central meridian of the sub-storm westward electrojet can be readily determined from the mid- and low-latitude magnetic observations (Kisabeth, 1972; Clauer and McPherron, 1974). Figure 2.8 shows the resulting horizontal magnetic perturbation vectors caused by a westward electrojet of 10^6 amps which is connected to a ring or cross-tail current via field-aligned currents (after Kisabeth 1972). An infinitely conductive layer was assumed at a depth of 250 km below the earth's surface to simulate induction effects for the calculation of the perturbation vectors. It can be seen in this figure that the mid-latitude stations are a strong indicator of the position of the central meridian, which in this case occurs at 270°. The mid-latitude horizontal magnetic perturbation vectors tend to point towards the central meridian by having their eastward components point in opposite directions on opposite sides of the central meridian.

If the baseline or zero level of each of the magnetic components is chosen just prior to the onset of each of the four events, then the ensuing mid-latitude H and D magnetic variations for Day 357 can be used to study the motion of the central meridian during each of the four events. The choosing of a baseline just prior to the onset

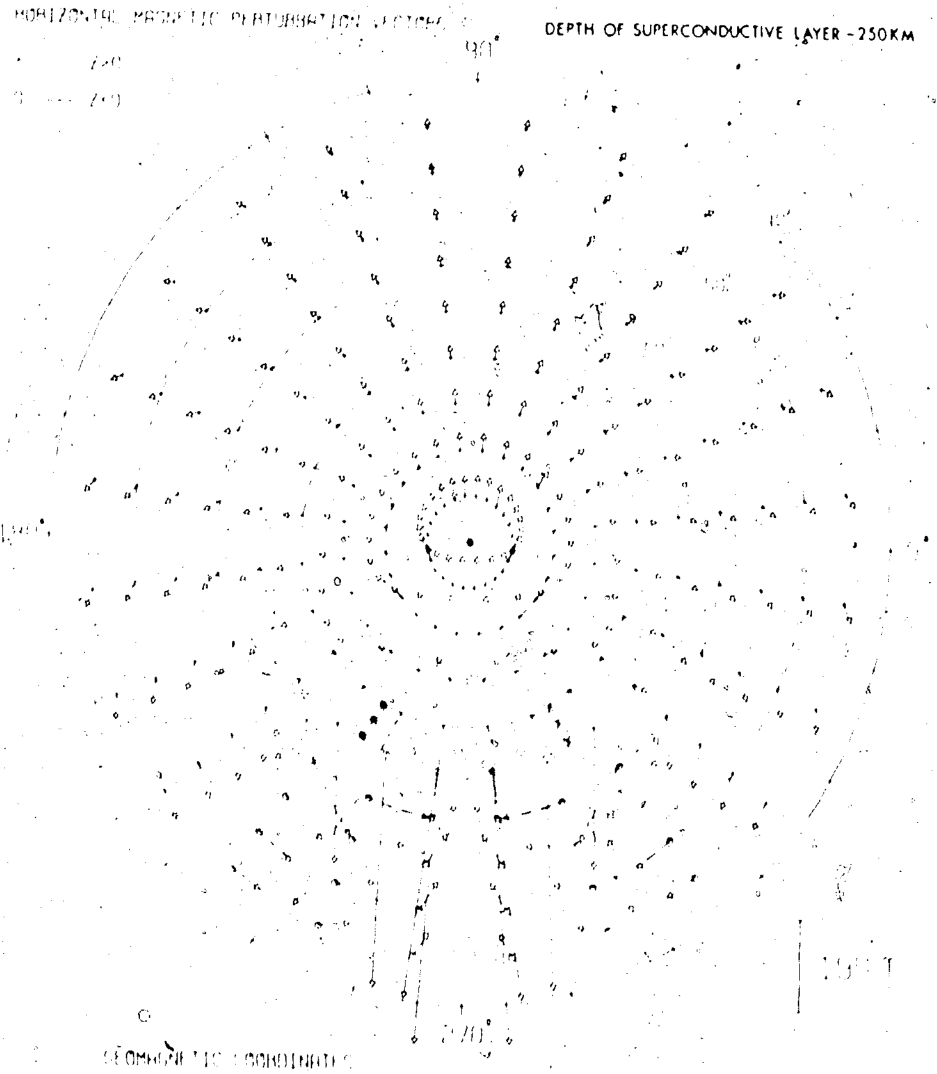
HORIZONTAL MAGNETIC PERTURBATION VECTORS
DEPTH OF SUPERCONDUCTIVE LAYER - 250KM
90°
180°
270°
GEOMAGNETIC COORDINATES

Figure 2.8

of a particular event largely reduces the effects of any previously existing electrojet thus allowing the development in the substorm [illegible]ent system from the time of onset of that given ev[illegible] be more clearly seen. It should be noted that the above method is limited by the assumption that the current system which develops after each onset consists primarily of a simple westward electrojet in a Birkeland current loop and implies the continued existence of the pre-onset current system. If, for instance, after a given onset an eastward electrojet were also to develop this would cause a shift in the mid-latitude horizontal magnetic perturbation vectors and would lead to an inaccuracy in the determination of the central meridian of the westward electrojet. However as Figures 2.2 and 2.4 show, the development of the westward electrojet during an event was always much larger than the corresponding development in the eastward electrojet during the same event. Thus for Day 357 it is possible to ignore the effects of the eastward electrojet and therefore use the mid-latitude horizontal magnetic perturbations vectors as indicators of the position of the central meridian of the westward electrojet.

Figures 2.9-2.12 present pairs of polar plots of the resulting horizontal magnetic perturbation vectors for each of the four events A, B, C and D. For each event a baseline was chosen just prior to the onset of the

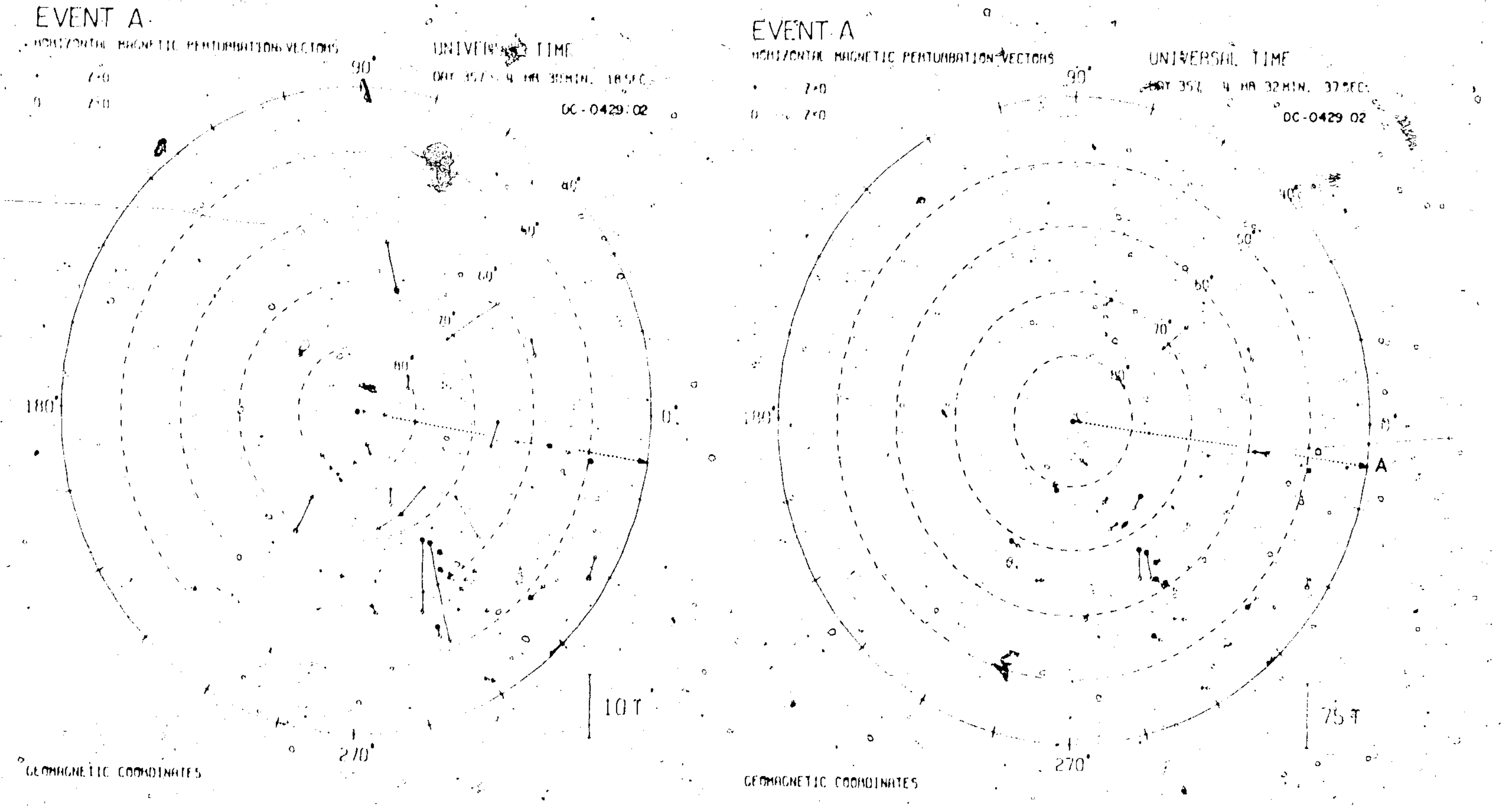
EVENT A
HORIZONTAL MAGNETIC PERTURBATION VECTORS
• Z>0
o Z<0
UNIVERSAL TIME
DAY 357 4 HR 30MIN. 18SEC.
DC-0429:02
90°
180°
0°
270°
40°
50°
60°
70°
80°
10 T
GEOMAGNETIC COORDINATES
EVENT A
HORIZONTAL MAGNETIC PERTURBATION VECTORS
• Z>0
o Z<0
UNIVERSAL TIME
DAY 357 4 HR 32MIN. 37SEC.
DC-0429 02
90°
180°
0°
270°
40°
50°
60°
70°
80°
A
75 T
GEOMAGNETIC COORDINATES

Figure 2.9

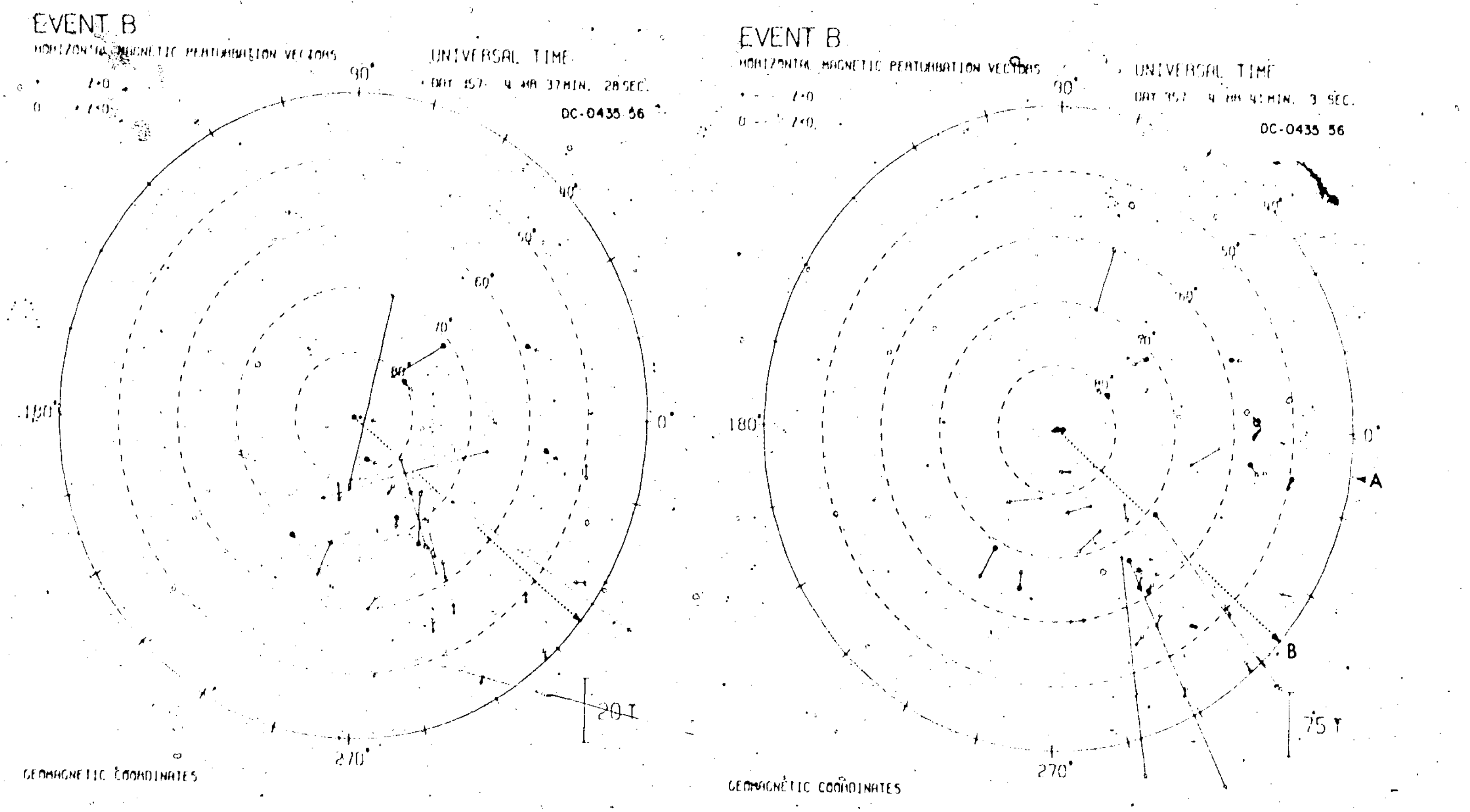
EVENT B
HORIZONTAL MAGNETIC PERTURBATION VECTORS
Z>0
Z<0
UNIVERSAL TIME
DAY 157 4 HR 37MIN. 28SEC.
DC-0435 56
90°
0°
180°
270°
40°
50°
60°
70°
80°
20 γ
GEOMAGNETIC COORDINATES
EVENT B
HORIZONTAL MAGNETIC PERTURBATION VECTORS
Z>0
Z<0
UNIVERSAL TIME
DAY 157 4 HR 41MIN. 3 SEC.
DC-0435 56
90°
0°
180°
270°
40°
50°
60°
70°
80°
A
B
75 γ
GEOMAGNETIC COORDINATES

Figure 2.10

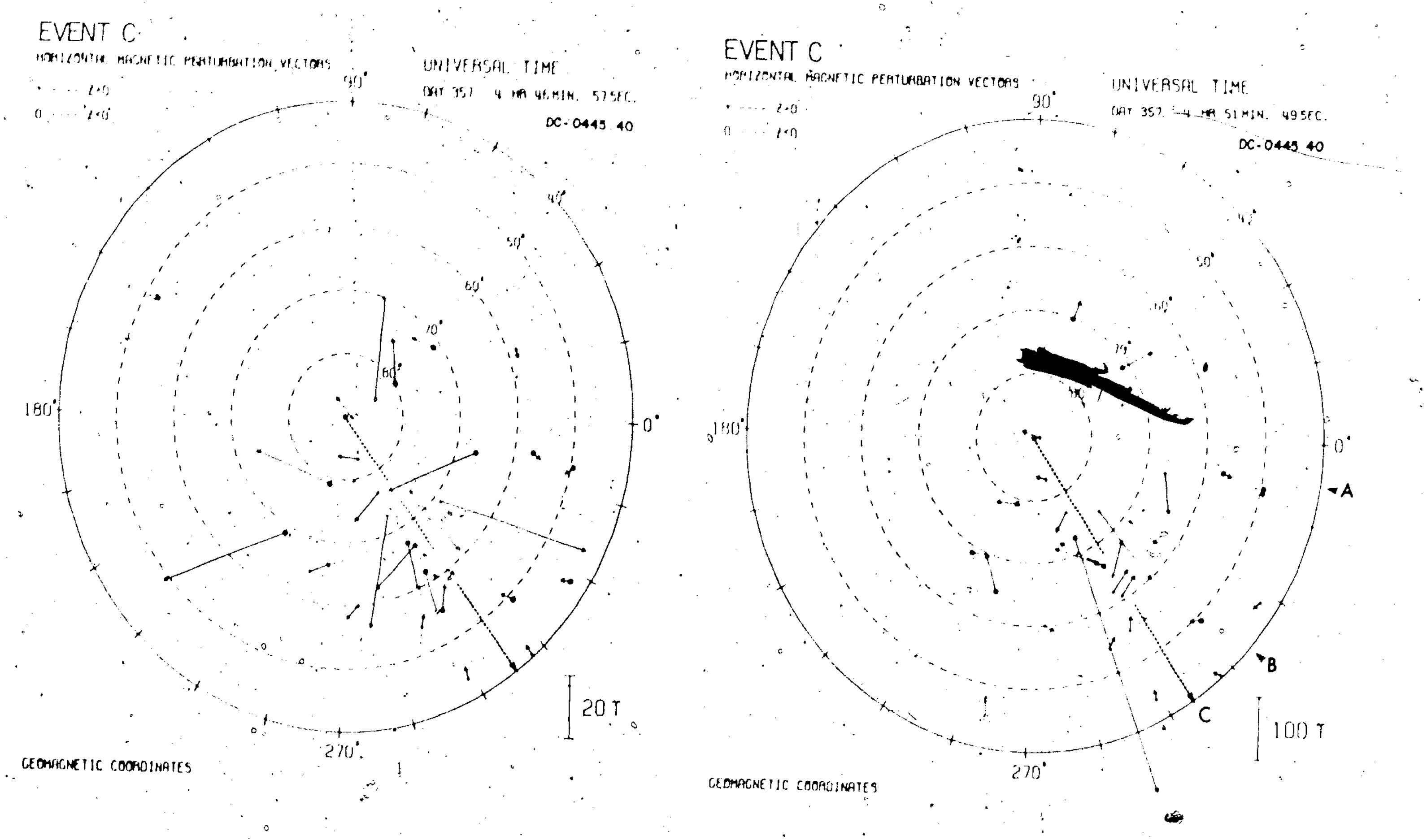
EVENT C
HORIZONTAL MAGNETIC PERTURBATION VECTORS
Z>0
Z<0
UNIVERSAL TIME
DAY 357 4 HR 46 MIN. 57 SEC.
DC-0445 40
90°
40°
50°
60°
70°
80°
180°
0°
270°
20 T
GEOMAGNETIC COORDINATES
EVENT C
HORIZONTAL MAGNETIC PERTURBATION VECTORS
Z>0
Z<0
UNIVERSAL TIME
DAY 357 4 HR 51 MIN. 49 SEC.
DC-0445 40
90°
40°
50°
60°
70°
80°
180°
0°
270°
A
B
C
100 T
GEOMAGNETIC COORDINATES

Figure 2.11

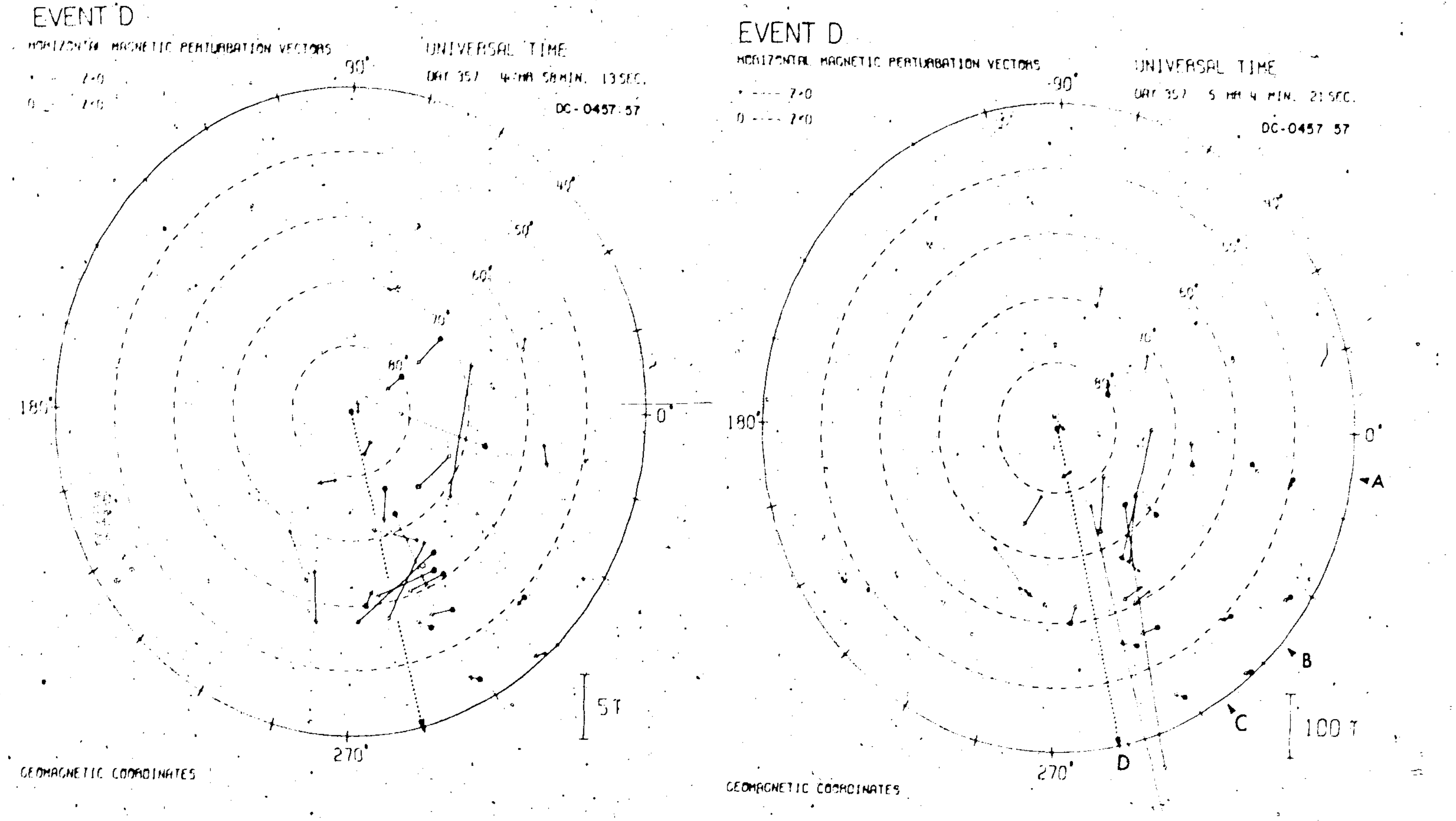
EVENT D
HORIZONTAL MAGNETIC PERTURBATION VECTORS
• ---- Z>0
0 ---- Z<0
UNIVERSAL TIME
DAY 357 4 HR 58 MIN. 13 SEC.
DC-0457 57
90°
0°
180°
270°
40°
50°
60°
70°
80°
5 T
GEOMAGNETIC COORDINATES
EVENT D
HORIZONTAL MAGNETIC PERTURBATION VECTORS
• ---- Z>0
0 ---- Z<0
UNIVERSAL TIME
DAY 357 5 HR 4 MIN. 21 SEC.
DC-0457 57
90°
0°
180°
270°
40°
50°
60°
70°
80°
A
B
C
D
100 T
GEOMAGNETIC COORDINATES

Figure 2.12

particular event and polar plots were drawn of the resulting horizontal magnetic perturbation vectors just after the onset and a few minutes later near the maximum of each event. The central meridian was determined for each of these two times from the mid-latitude stations and is indicated by the dotted line in each of the polar plots. The error of each of these central meridians is approximately ± 3 degrees. For the subsequent events, B, C and D (Figures 2.10-2.12), the positions of the central meridians associated with the maxima of the previous events are indicated by the respective arrows on the outside perimeter of the polar plot. It is evident from these figures that during each of the events the movement of the central meridian was small, averaging about three degrees (which is of the order of the error involved) while the movement of the central meridian from event to event was large, averaging twenty degrees.

If the westward electrojet expanded continuously westwards during each of the events, then one would expect to see a shift of the central meridian between the onset and the maximum of the event which was comparable to the shift in the central meridian from event to event. Since this is not the case it must be concluded that the motion of the westward electrojet was not continuous.

Thus for Day 357 the western end of the substorm westward electrojet was observed to expand to the northwest through a sequence of discrete jumps with each jump involving an onset of the substorm electrojet simultaneously over a broad region. For Day 357 the first onset in the sequence occurred near midnight in the WHAL region while the last westward jump occurred in the CAMB region at about 0500 UT. The jumping of activity westwards ceased at this time; however, for the next $1\frac{1}{2}$ hours the high-latitude stations (RESO, CONT, BAKE) in the regions of previous electrojet intensifications showed continued activity. Figure 2.13 illustrates schematically estimates of the positions of each of the steps involved with the expansion of the western end of the substorm electrojet. We wish to emphasize here that the network of observatories used in this study does not permit us to accurately determine the eastern extremity of the electrojet. Therefore, this schematic diagram is only meant to illustrate qualitatively the poleward and westward motion of the western end of the substorm disturbed region. What happens in the morning sector at the times of these westward expansions in the evening sector cannot be determined from the data suite used in this study.

DAY 357

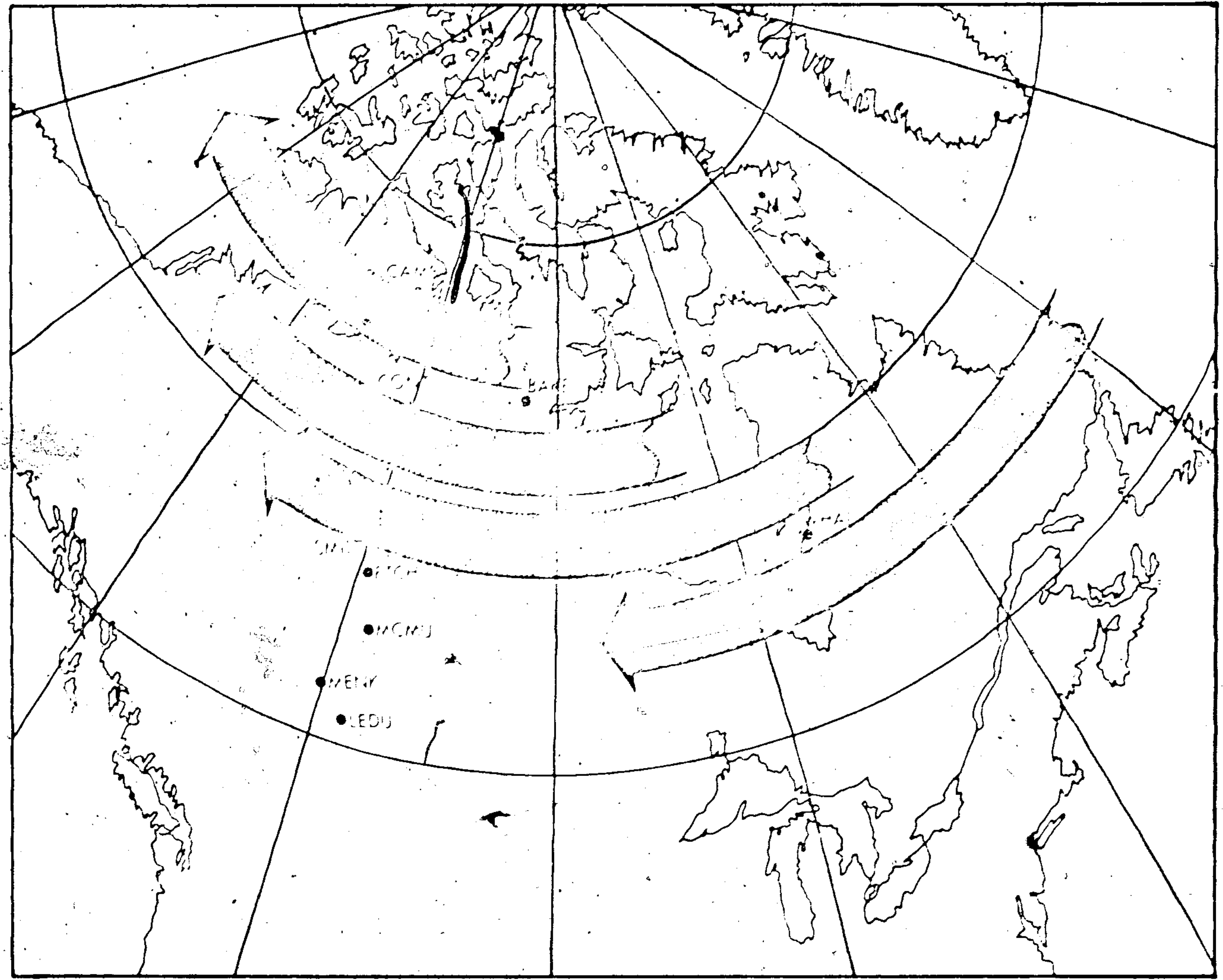

Figure 2.13

2.4 Study of Westward Jumping of Substorm Electrojet Activity on Day 329, 1971

On November 25, 1971 (Day 329) another example of what has been termed a [illegible] (that is a substorm which expands to the northwest through a series of discrete jumps) occurred between 0415 and 0500 UT. The magnetic variations in the H component for mid- and low-latitude stations are shown in Figure 2.14. The data from the stations in Figure 2.14 are again arranged in an east to west manner so that the most easterly station is situated at the top of the figure.

Figure 2.14 shows a series of six onsets (labeled A through F) which have been identified between 0415 and 0500 UT. The first of these onsets (event A) occurs at 0416 UT. At this time FARA, JUAN and HUAN all show the onset of a positive H slope (which is the previously discussed mid-latitude signature for the onset of a substorm westward electrojet). Also at the time of the onset of event A, DALL (which is just to the west of HUAN) enters an indecisive state showing neither a marked onset of a $+\Delta H$ nor the continuation of the growing negative H. The remaining stations to the west of DALL all show either an onset or continuation of a $-\Delta H$ trend, indicating the continued development or growth of upward field aligned current to the east of these stations.

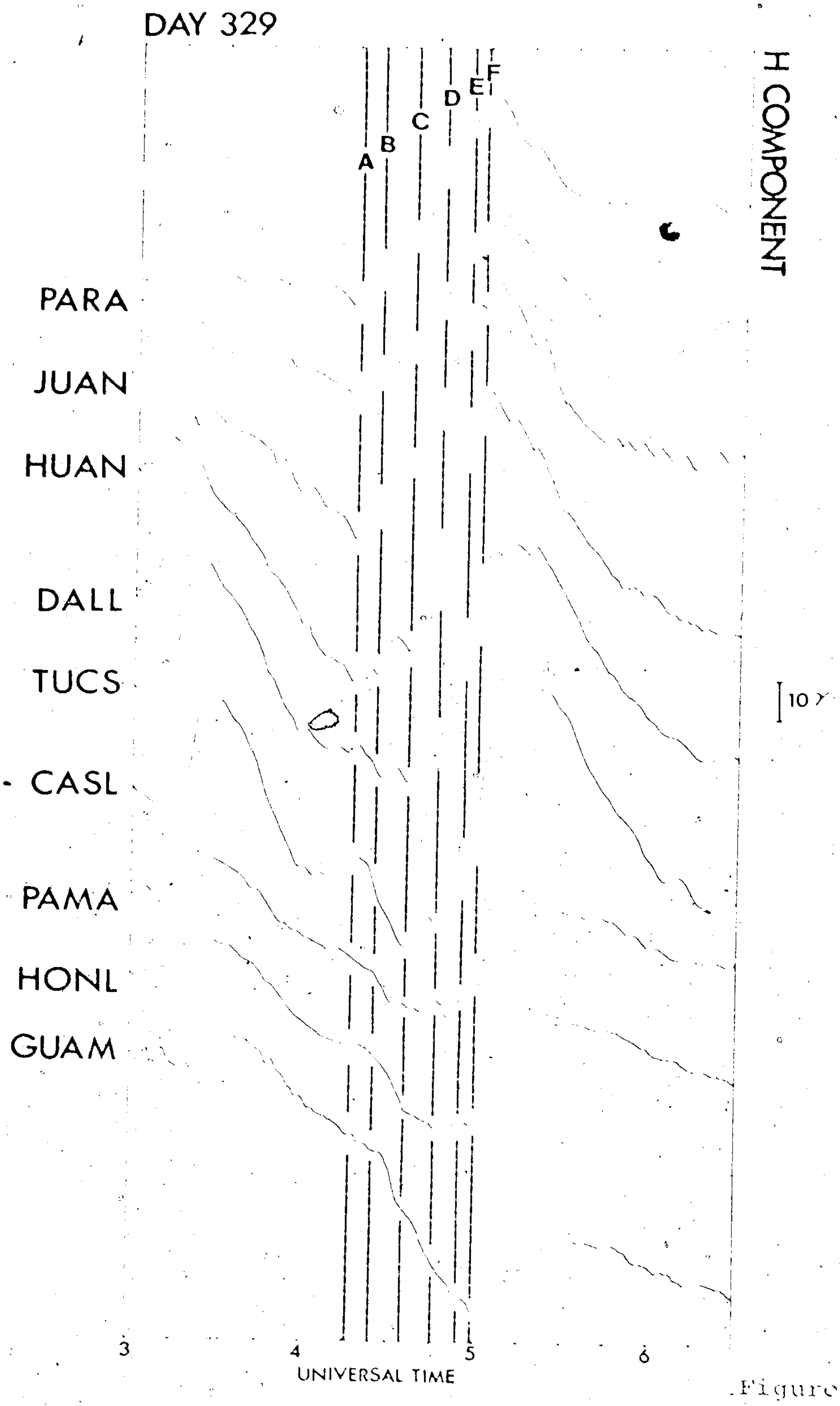
DAY 329
A
B
C
D
E
F
H COMPONENT
PARA
JUAN
HUAN
DALL
TUCS
CASL
PAMA
HONL
GUAM
10γ
3
4
5
6
UNIVERSAL TIME

Figure 2.14

Ten minutes later, at 0425 UT, a mid-latitude onset (event B) is observed at DALL while TUCS (which is just to the west of DALL) now enters an indecisive state. A clear enhancement in the growth of negative H occurs at this time for the stations located to the west of TUCS.

The next onset (event C) is observed at 0435 UT at TUCS and CASL with the stations to the west of CASL showing continued growth of negative H. At 0446 UT a marked positive inflection is observed in the H component of CASL (event D) while PAMA and HONL show an indecisive behaviour at this time. Events A through C show that when an initial onset of a $+\Delta H$ occurs in a given sector that it is seen at mid-latitude stations to the east of that sector as an intensification or inflection in the already positive trending H. Thus the inflection at CASL suggests that, corresponding to event D, a narrow sector between CASL and PAMA experienced an initial onset of $+\Delta H$. Confirmation that an onset did indeed occur at the time corresponding to the inflection at CASL will be obtained from the high-latitude magnetic observations (which will be discussed later in this section). Further initial onsets of a $+\Delta H$ are observed at 0454 UT at PAMA (event E) and at 0459 UT at HONL and GUAM (event F).

The mid-latitude observations indicate that a series of six substorm onsets took place between 0415 and 0500 UT. The fact that each onset occurred at a station which was to the west of the previously recorded onset reveals the substorm disturbance was moving westwards. If the westward expansion of the substorm electrojet was continuous in character, then one would expect to see an observable lag in the onset time between any two adjacent (but widely separated) stations. However for some of the events, initial onsets were observed simultaneously at more than one station. Moreover, when a mid- or low-latitude station experienced its initial onset of a $+\Delta H$ simultaneous positive inflections were also seen in the H component of those stations to the east which had previously experienced an initial onset. If the mid-latitude station experiencing its initial onset was just one point in the path of a continuously westward expanding region of substorm activity there would be no reason for this onset to show up as an inflection in the H component for those stations situated to the east. Thus, the jump-like character of the mid-latitude onsets taken together with the observed inflections to the east suggests that the westward propagation of substorm activity was not continuous but rather that the region experiencing substorm activity expanded westwards through a series of six discrete jumps or steps.

Figure 2.15 shows the H or X component of the high-latitude stations which experienced an onset of a substorm westward electrojet during the interval 0400 UT-0600 UT on Day 329. The times of occurrence of the six onsets determined from the mid- and low-latitude stations are indicated on Figure 2.15 by the respective dashed lines. It can be seen that, corresponding to the first onset (event A) which was observed at PARA, JUAN and HUAN, an onset of a negative H was observed at WHAL. Furthermore, it can be seen from Figure 2.16, which shows the Z component for WHAL, that the onset of $-\Delta H$ at WHAL coincides with the onset of a $+\Delta Z$ at that station. The $-\Delta H$ implies that WHAL was in the region of an intensified westward electrojet while the $+\Delta Z$ indicates that the center of this electrojet was to the south of WHAL. CHUR X shows no marked trend at this time while the H component at NARS shows a confused but basically negative trend. Thus, corresponding to the event A observed in the mid-latitude stations, a substorm westward electrojet onset occurred to the southeast of WHAL.

The second event (event B), corresponding to the initial onset at DALL, coincides with the onset of a $-\Delta H$ at

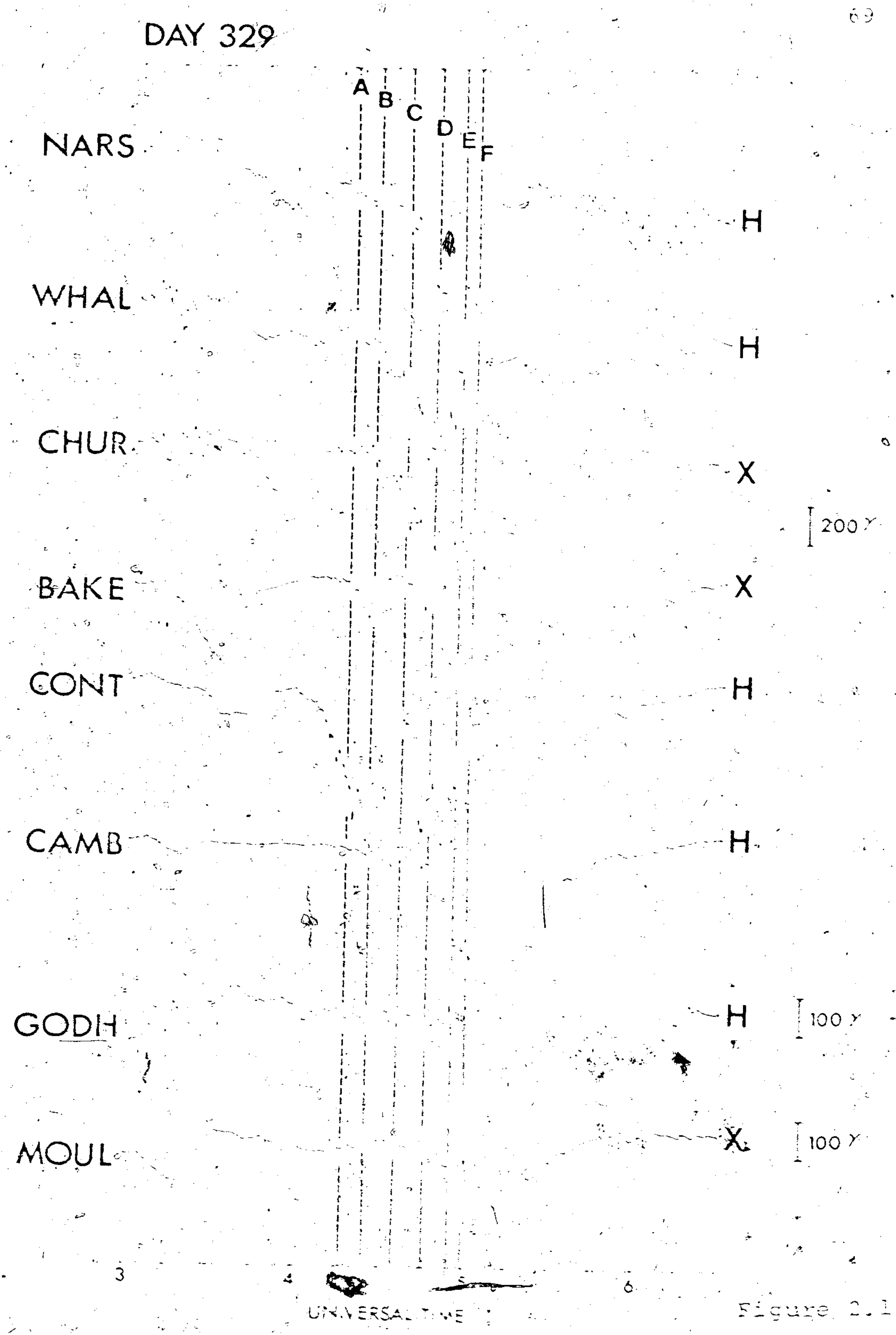
DAY 329
A
B
C
D
E
F
NARS
H
WHAL
H
CHUR
X
200 γ
BAKE
X
CONT
H
CAMB
H
GODH
H
100 γ
MOUL
X
100 γ
3
4
5
6
UNIVERSAL TIME

Figure 2.15

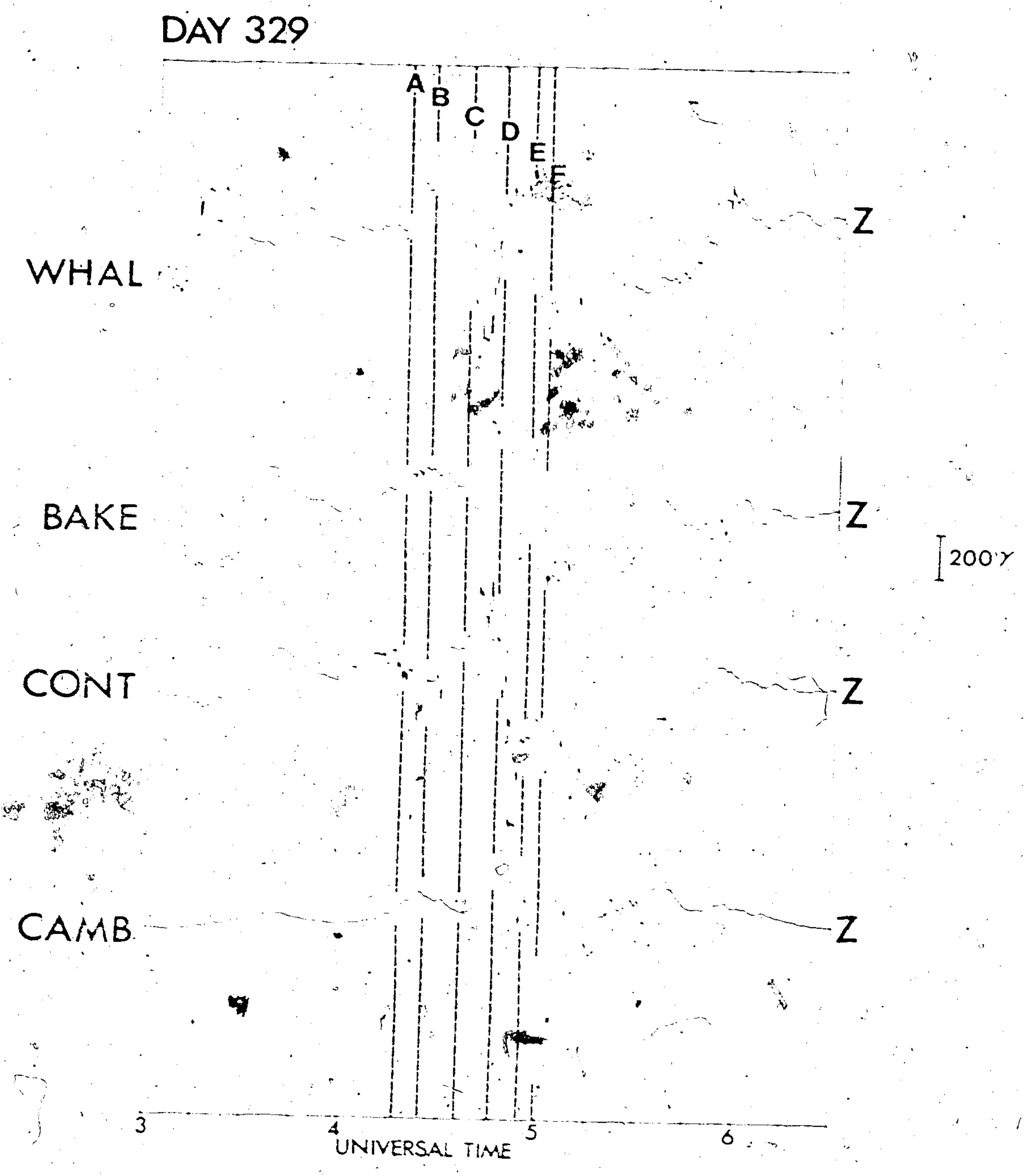
DAY 329
A
B
C
D
E
F
WHAL
Z
BAKE
Z
200γ
CONT
Z
CAMB
Z
3
4
5
6
UNIVERSAL TIME

Figure 2.16

CHUR (Figure 2.15) and with an intensification of negative H at WHAL. The WHAL Z component (Figure 2.16) also shows a strong positive intensification at the time of onset of event B. Therefore, in conjunction with the observed onset at BALL, the onset of a second substorm westward electrojet is observed in the CHUR-WHAL region. The strong positive Z intensification at WHAL implies that the bulk of the second current system is still south of WHAL.

At the time of the third event (event C) corresponding to the initial onset of a positive H bay at TUCS and CASL, an onset of negative H is observed at BAKE and CONT (Figure 2.15). The onset of negative H at BAKE and CONT implies the development of a third westward electrojet to the west of the two previous current systems. Examining Figure 2.16 it is seen that the WHAL Z component shows a strong negative change at this time, indicating that the position of this, the third westward electrojet in the sequence so far, is to the north of WHAL, and is thus to the north of the two previous electrojets. Both BAKE and CONT show a strong positive change in the Z component which places the center of this new electrojet just south of these two stations. Looking again at the H component for CONT (Figure 2.15) it is seen that CONT experienced two separate onsets of negative H bays in close succession. The first onset occurred at 0405 UT several minutes prior to event A in the substorm sequence. The second onset at CONT occurred in conjunction with event C as described above. It should be pointed out that the first onset at CONT is not part of the substorm sequence. The first onset at CONT was due to a relatively confined substorm since the mid-latitude observations (Figure 2.14) indicate that the only station showing a noticeable positive trend in H at the time of this first onset was CASL. Thus the magnetic observations suggest the following picture. A localized substorm occurred in the CONT region prior to the onset of the substorm sequence. At about 0418 UT, a [illegible]storm commenced far to the south-east of CONT. This substorm developed into a substorm sequence with substorm activity propagating to the north-west through a series of discrete jumps. In association with the third jump in this sequence the substorm westward electrojet entered the CONT region at which time CONT experienced a second onset.

Associated with the fourth mid-latitude onset (event D) is the onset of a negative H bay at CAMB (Figure 2.15). The CAMB Z component (Figure 2.16) shows a positive intensification at this time while an onset of negative Z occurred at CONT in conjunction with event D. Thus the position of the center of this fourth substorm westward electrojet is to the north of CONT and to the south of CAMB.

At the time of event E, corresponding to the onset in the [illegible] region, onsets of negative H bays are observed at GDHN and MOUL. Figure 2.17 presents the Z components for GDHN, RESO and MOUL. All three stations show a positive Z enhancement at the time of onset of event E indicating that the center of the fifth electrojet to develop is to the south of all three of these stations. The −Z at CAMB (Figure 2.18) indicates that the center of the fifth electrojet is to the north of CAMB.

The final event (event F), which corresponds to the initial bays at MOUL and GDHN, coincides with enhancements of positive Z at RESO and MOUL (Figure 2.17) while GDHN shows an onset of a negative trending Z at this time. Thus the sixth and last observed electrojet to develop is still positioned to the south of MOUL and RESO but is now north of GDHN.

Figure 2.18 presents schematically, estimates of the position of each (events A through F) of the six step-like expansions into the evening sector of the substorm westward electrojet. It should be realized that this diagram is qualitative since there is insufficient station coverage to determine accurately the length and width of each current system. However, it is still possible to see some of the grosser features in the development of the

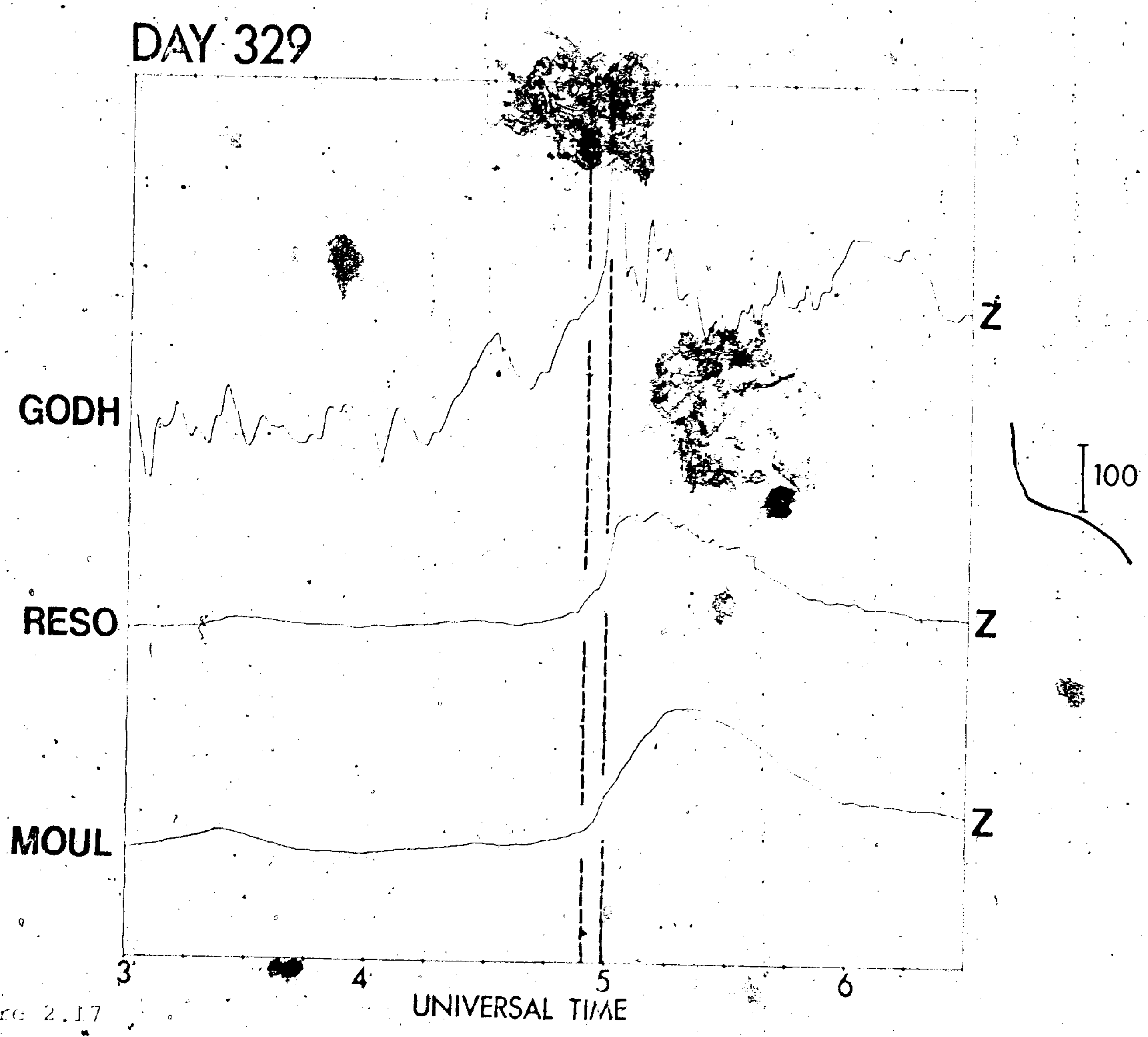

gure 2.17

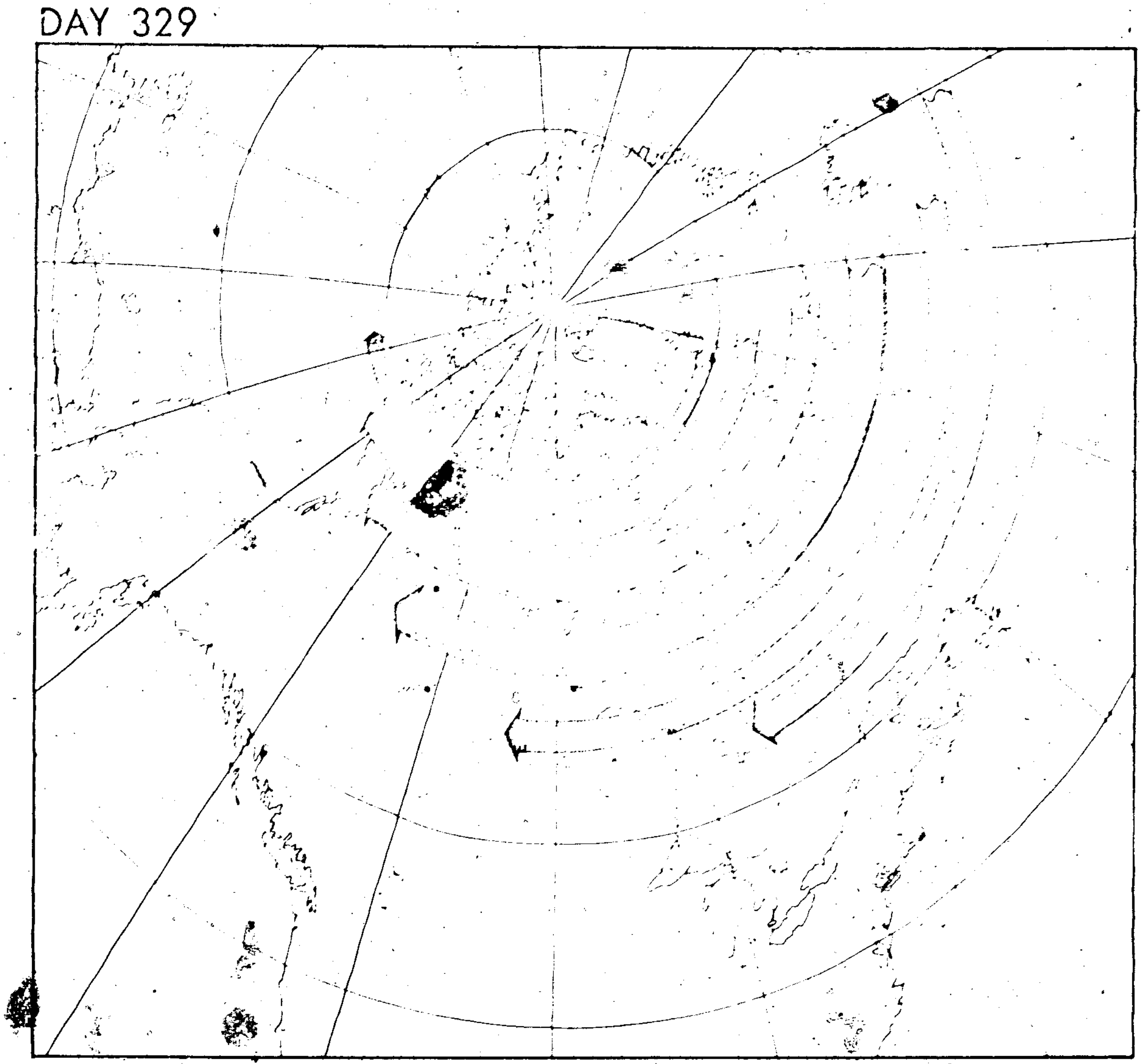

Figure 2.18

substorm sequence for Day 329. One feature to be noted is that the strengths of the last two current systems to develop, as seen by the depth of the negative H bays at MOUL and GOPH, are considerably reduced in comparison to the previous electrojets in the substorm sequence.

2.5 Study of Westward Jumping of Substorm Electrojet Activity on Day 328, 1971

Another example of a westward stepping substorm electrojet occurred on November 24, 1971 (Day 328), between 0430 and 0530 UT. Figure 2.19 shows a sampling of the observations for the period 0330 to 0630 UT. The two groups of stations (the high and lower latitudes) are each arranged in the previously described east-west manner. Looking first at the mid- and low-latitude stations in Figure 2.19 it can be seen that at 0430 UT, HUAN, FRED, DALL and TUCS all experienced an onset of +H (event A) while [illegible] west of TUCS both CASL and HONL show a continued growth [illegible] negative H. TAMA, which is located in the southern hemisphere, shows no marked trends at this time. Thus the mid- and low-latitude stations indicate that a substorm onset occurred at this time in the sector stretching from HUAN to TUCS while growth of negative H continued to the west of TUCS. The high-latitude observa-

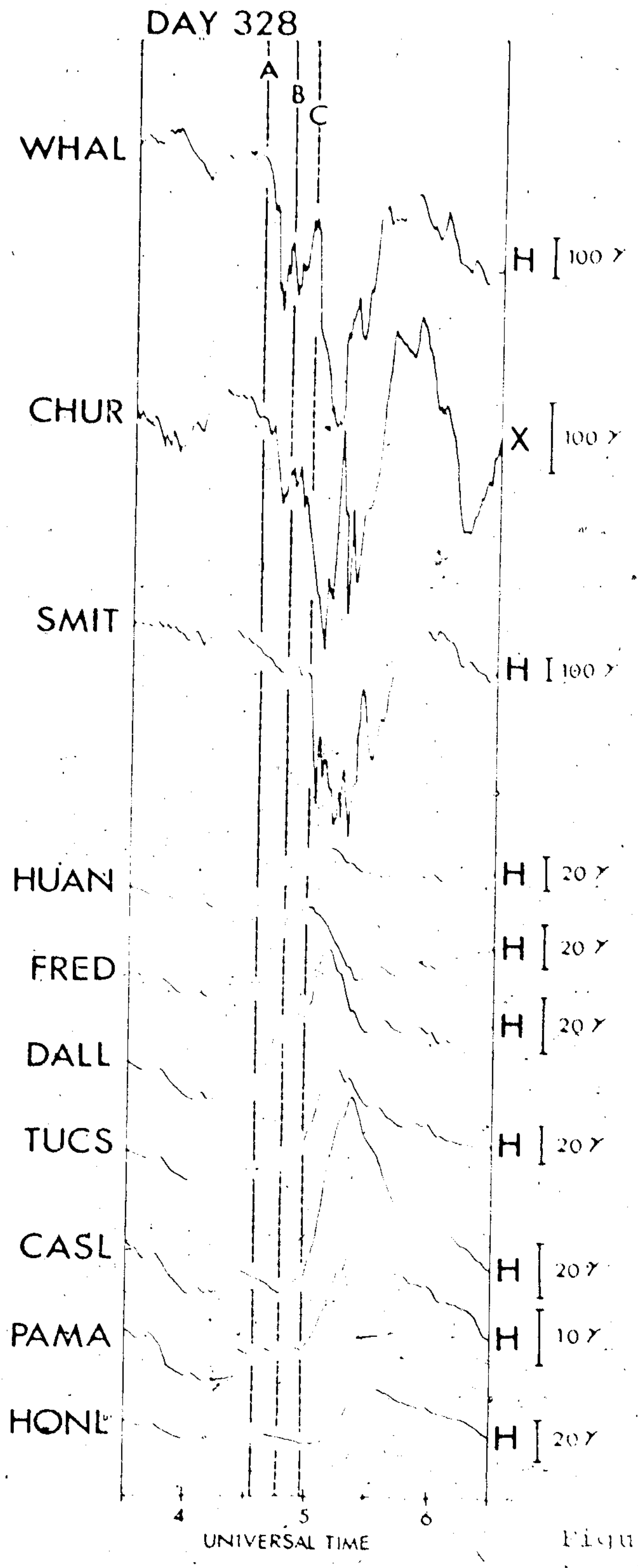
DAY 328
A
B
C
WHAL
H
100 γ
CHUR
X
100 γ
SMIT
H
100 γ
HUAN
H
20 γ
FRED
H
20 γ
DALL
H
20 γ
TUCS
H
20 γ
CASL
H
20 γ
PAMA
H
10 γ
HONL
H
20 γ
4
5
6
UNIVERSAL TIME

Figure 2.19

tions for this time show that corresponding to the mid-latitude onset (event B) described above, an onset of a negative H bay occurred in the WHAL-CHUR region.

CASL continues to show growth until 0446 UT at which time it experiences a weak onset of a +H (event [illegible]). BOSL continues to show a growth in negative H at this time. None of the high-latitude stations used in this study experienced an initial onset of a negative H at this time. There is, however, a large gap in the high-latitude station coverage between CHUR and SMIT, which is the region where the substorm westward electrojet associated with event B would be expected. Moreover the rate of change of H at CASL was small, suggesting that the electrojet which developed in association with event B was a relatively weak one which would further hinder efforts to locate the signature in an auroral zone station. There is, however, an intensification in the current system at both WHAL and CHUR (Figure 2.19), in conjunction with event B, implying that the mid-latitude onset associated with event B was the result of a substorm westward electrojet onset or intensification which occurred once again in the WHAL-CHUR region.

At 0458 UT an initial onset of a +H was observed at PAMA (event C) along with strong intensifications [illegible] positive H at DALL, TUCS, and CASH. HONL stops growing at this time and enters an indecisive state. Corresponding precisely to this low latitude onset is a sharp onset of a negative H bay at SMIT. Event C is associated with an onset of −H at SMIT (Figure 2.20) and a weaker onset of −H at CONT. These observations place the center of the third substorm electrojet somewhere to the north of SMIT and south of CONT. The weaker onset of a −H at CONT suggests that CONT is only seeing the distant effects of the electrojet while the sharp onset at SMIT places that station much closer to the electrojet.

At 0509 UT HONL experienced an initial onset of +H (Figure [illegible]). At the time of this onset (event D) CONT experienced a [illegible] intensification in both H and Z. The intensification of −H at CONT is again indicative of an electrojet onset which has occurred out of the region of the station. However the intensification in the Z component, resulting in a still larger ΔZ suggests that this electrojet is closer to CONT than the previous electrojet associated with event C.

Finally at 0517 UT both PAMA and HONL experience an inflection or intensification in their already existing positive H bays (event E), suggesting the onset of a mid-latitude positive H bay at stations situated further to the

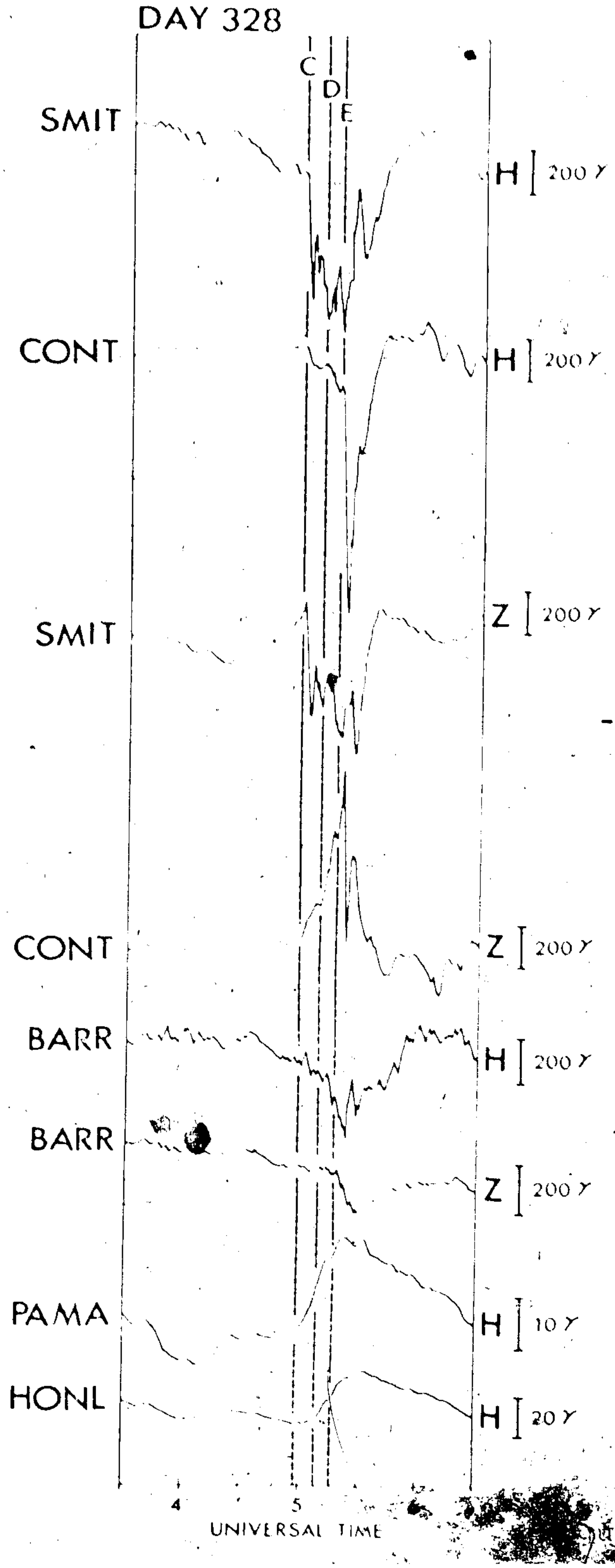
DAY 328
C
D
E
SMIT
H 200 γ
CONT
H 200 γ
SMIT
Z 200 γ
CONT
Z 200 γ
BARR
H 200 γ
BARR
Z 200 γ
PAMA
H 10 γ
HONL
H 20 γ
4
5
UNIVERSAL TIME

west (Figure 2.20). Corresponding to this mid latitude onset is the strong onset of a negative H bay at CONT. A strong intensification of the Z also occurred at this time. Thus the H and Z components at CONT and [illegible] the sudden development of a substorm westward electrojet with the northern edge of the current system located near CONT.

Figure 2.21 presents an estimate of the location and extent of the regions associated with each of the step like expansions of the western end of the substorm electrojet. Note that the configuration of the last two electrojets, associated with events D and E, agree with the observations at BARR (Figure 2.20). For the electrojet associated with event D one would expect a weak +H with little change in Z at BARR while for the last onset (event E) one would expect to see a slight intensification of the +H along with a weak +Z which is what is observed.

The mid- and high-latitude magnetic observations for Day 328 suggest that an initial substorm onset occurred at about 0430 UT in the WHAL region. This substorm then proceeded to develop to the northwest through a series of five discrete jumps with each jump being associated with an onset of a substorm westward electrojet.

DAY 328

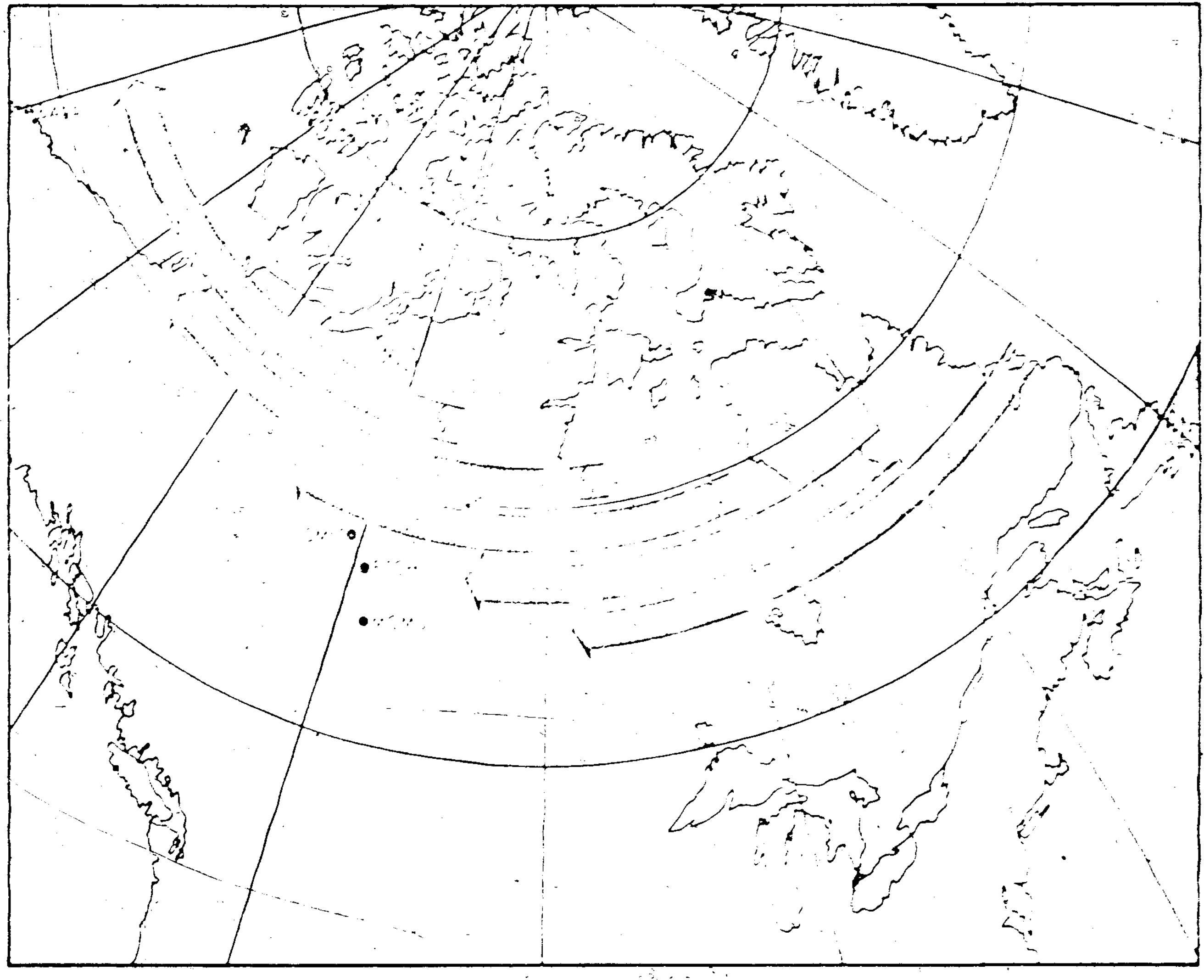

Figure 2.27

CHAPTER III

DISCUSSION AND CONCLUSIONS

3.1 Summary and Discussion of Evidence for the Westward Jumping of Substorm Activity

On the basis of the three polar magnetic substorms analysed in this thesis, it has been concluded that the propagation of the substorm westward electrojet through the evening sector takes place as a series of discrete northwest jumps or steps. The mid- and low-latitude observations which led to the above conclusion are: (1) Mid-latitude onsets of positive H bays occurred in succession with the sectors to the east experiencing onsets before the sectors to the west. (2) For several of the events, adjacent but widely separated stations showed simultaneous onsets. (3) Coinciding with an initial onset in any given sector positive inflections or intensifications in H were observed at mid-latitude stations positioned to the east of that sector. (4) Mid-latitude stations to the west of the sector experiencing its initial onset simultaneously experienced an intensification in the growth of negative H. This last observation implies that an impulsive increase in the field aligned current at the western edge of the sector experiencing the expansive phase, which is in agreement with the synchronous satellite observations presented by Lezniak and Winkler (1970). These authors concluded that there is a fault line, west of which substorms are accompanied by geomagnetic inflation and east of which they are accompanied by a collapse.

High-latitude magnetic observations also gave a strong indication of the impulsive nature of the westward propagation of substorm activity. (1) The onsets of high-latitude intense negative bays were observed to occur in succession with regions to the southeast experiencing onsets before the regions to the northwest. (2) In association with each high-latitude onset, inflections were observed in the magnetic components at both stations to the northwest which had not as yet experienced an onset and at the stations situated to the southeast which had already undergone initial onsets of intense negative bays. This observation, as in the mid- and low-latitude case, strongly suggests that the westward motion of bay activity is not continuous, for if the onset at any given station is simply the result of a continuously westward expanding region of substorm activity which finally expands over the station in question, then there would be no reason for corresponding impulsive intensifications or inflections to occur at stations situated outside of the immediate region experiencing its initial onset. (3) Onsets of intense negative bays were also observed to occur simultaneously at widely separated stations. First one group of stations would simultaneously experience an onset then some time later a second group of stations, situated to the northwest of the first group, would experience simultaneously an initial onset. Again, as in the mid- and low-latitude case, these observations strongly suggest that the region of intense negative bays is not expanding continuously westwards since if this region was expanding continuously one would expect to see some time lag between the onset of a negative bay for adjacent but widely separated stations. (4) The time of occurrence of each high latitude onset was found to closely coincide to the time of occurrence of the corresponding mid-latitude onset. This observation further strengthens the idea that the observed westward jumping of mid-latitude onsets can be taken as evidence of the westward jumping of substorm activity in the high latitude region.

Thus the picture evolved from the analysis of these substorms is one in which a sudden onset of substorm activity occurs in a localized longitudinal and latitudinal sector so that while energy is being dissipated rapidly in the expansive phase sector, it is being stored in adjacent sectors to the west and thus making conditions ripe in these westward sectors for an expansive phase onset which in turn feeds or sets up sectors still further to the west. So, in this picture, sectors in the ring or cross-tail current collapse in succession with each sector collapse perturbing a localized region on the Earth across which intense initial onsets of negative H bays occur simultaneously. The whole picture as viewed from the ground appears as a sequence (which we have termed a substorm sequence) of westward electrojets. These electrojets develop in succession at intervals of approximately 5-15 minutes, in such a way that the region experiencing substorm westward electrojet activity expands to the northwest through a series of discrete steps or jumps.

3.2 Physical Significance of Jumping of Substorm Activity

The question arises regarding the physical significance of the stepwise development of the substorm westward electrojet. The answer may lie in the self-inductance of the substorm current system which governs the rate of change of current in the substorm electrojet which in turn determines the rate at which energy can be dissipated by this current system. Rostoker and Boström (1976) have shown that the quiet time electrojet has a time constant $\tau = L/R$ of about 50 minutes, where L is the self-inductance of the circuit and R the ohmic resistance. Thus if the change in current which occurs during a substorm was simply an intensification and expansion of the quiet electrojet then changes in the substorm current system would take place with a time constant of the order of 50 minutes. This certainly is not what is observed, as can readily be seen from the events presented in this thesis, the substorm current system fluctuations are of the order of a few minutes not several tens of minutes. This suggests that self-inductance may be playing a role in limiting the scale size of the substorm current system.

The process which leads to the development of a succession of several small substorm current systems rather than one large one could be that of a plasma instability in the tail which triggers a sudden release of energy. The energy released is dissipated in part in the form of joule heating in the ionosphere through the development of a direct current which flows through the resistive ionosphere. This ionospheric current would, of course, be linked to the magnetosphere by field-aligned currents.

Since energy in the tail is stored primarily in the magnetic field, disruption of the tail current through a plasma instability would demand an immediate release of magnetic energy. The dissipation of energy by the substorm current circuit must then be very rapid to be consistent with the rate of energy release in the tail. Thus a sudden release of energy in the tail would tend to favour a limited scale size for the substorm current circuit which develops, since the circuit must have a relatively small self-inductance in order to permit rapid change of current in the circuit.

If the instability which triggers the release of energy in the tail propagates westwards and triggers further energy releases, as one might expect if the perturbation stems from a drift wave instability, then further substorm current circuits of limited size must be set up to dissipate this energy. The time between substorm intensifications would thus reflect the time required for the longitudinal sector adjacent to a substorm disturbed region to become unstable. The net result would be that the substorm westward electrojet would appear to propagate westwards in a step-like fashion.

3.3 Implications of Jumping of Substorm Activity on a Growth Phase

The final point which we wish to discuss has to do with the relation of the growth phase to the expansive phase. Previous workers (Belyakova et al., 1968; McPherron, 1970; Iijima and Nagata, 1972) have described such characteristics as a decrease in the H component at mid-latitudes or a slight decrease in the H component at high-latitudes before an intense onset as signatures of a growth phase. The mid-latitude observations presented in this thesis clearly indicate that when a mid-latitude onset of +ΔH occurs in one sector then there is a concurrent enhancement in the growth of -ΔH at mid-latitude stations to the west of that sector. This confirms the conclusions of many earlier workers (e.g. Fukushima, 1953; Akasofu and Meng, 1968) who using statistical and individual event studies, established the behaviour of low-latitude bays as a function of local time. The high-latitude observations also show that a gradual decrease in the H component before the sudden onset of a negative bay can be associated with negative bay onsets which occur in the region to the south-east of the station in question.

When the above features were attributed to growth the implication also seems to have been made that a growth phase existed which was a phenomenon which was independent of any other phase of the substorm in that it proceeded all of the other phases of the substorm. However as the observations presented here suggest, enhancement in the growth of negative [illegible] mid-latitudes may be directly associated with the onset of an expansive [illegible] the east while the gradual decrease in H at high-latitudes can probably be attributed to the station seeing an expansive phase current system which is in a region located to the southeast of the station.

We would like to emphasize that we are not invoking the above considerations to argue against the idea of a growth phase; we merely wish to point out that the fact that a particular magnetic signature took place in a sector before that sector experienced its onset does not <u>necessarily</u> mark that signature as a characteristic of pure growth since each sector is affected by what is going on in the adjacent sectors. Growth may indeed be going on in sectors to the west of the region experiencing its expansive phase <u>which would thus suggest that growth is not necessarily an independent phase</u>. The elusive growth phase which is defined as an independent part of the substorm which proceeds all other forms of substorm activity may not always exist. However if it does and one wishes to find its magnetic signature then one must be very careful to choose a time prior to the first onset in the substorm sequence since if one chooses a time prior to a subsequent onset but after the first onset then one runs into the inherent difficulty of whether the signature observed is one of growth or is the direct result of an expansive phase.

BIBLIOGRAPHY

Akasofu, S.-I., The development of the auroral substorm, [illegible], [illegible], 273, 1964.

Akasofu, S.-I., C.-I. Meng and D. S. Kimball, Dynamics of the aurora, IV, Polar magnetic substorms and westward travelling surges, [illegible], [illegible], 489, 1966.

Akasofu, S.-I. and C.-I. Meng, Low latitude negative bays, [illegible], [illegible], 227, 1968.

Akasofu, S.-I., Polar and Magnetic Substorms, D. Reidel Publ. Co., Dordrecht, Holland, 1968.

Akasofu, S.-I., Magnetospheric substorms: a model, in: Solar Terrestrial Physics/Leningrad, 1970, part 3, edited by E. R. Dyer and J. G. Roederer, p. 131, D. Reidel Publ. Co., Dordrecht, Netherlands, 1972.

Akasofu, S.-I. and S. Chapman , Solar Terrestrial Physics, Oxford Press, 1972.

Atkinson, G., A theory of polar substorms, *J. Geophys. Res.*, *71*, 5157, 1966.

Axford, W. I. and C. O. Hines , A unifying theory of high-latitude geophysical phenomena and geomagnetic storms, *Can. J. Phys.*, *39*, 1433, 1961.

Axford, W. I., The interaction between the solar wind and the earth's magnetosphere, *J. Geophys. Res.*, *67*, 3791, 1962.

Axford, W. I., H. E. Petschek and G. L. Siscoe , *J. Geophys. Res.*, *70*, 1231, 1965.

Bame, S.J., R. Asbridge, H. E. Felthauser, E. W. Hones and I. B. Strong, Characteristics of the plasma sheet in the earth's magnetotail, *J. Geophys. Res.*, *72*, 113, 1967.

Belyakova, S. I., S. A. Zaytseva and M. I. Pudovkin, Development of a polar storm, *Geomagn. Aeron., Engl. Transl.*, *8(4)*, 569, 1968.

Biermann, L., Solar corpuscular radiation and the interplanetary gas, [illegible], 109, 1957.

Birkeland, K., The Norwegian Polaris Expedition 1902-1903, Vol. 1, 1st. sec., Aschehoug and Co., Christiania, 1908.

Birkeland, K., The Norwegian Polaris Expedition 1902-1903, Vol. 1, 2nd. sec., Aschehoug and Co., Christiania, 1913.

Bonnevier, B., R. Boström and G. Rostoker, A three-dimensional model current system for polar magnetic substorms, *J. Geophys. Res.*, *75*, 197, 1970.

Cahill, L. J., The inflation of the inner magnetosphere during a magnetic substorm, *J. Geophys. Res.*, *71*, 4505, 1966.

Chapman, S. and V. C. A. Ferraro, A new theory of magnetic storms, *Terr. Magn. Atmos. Elec.*, *36*, 77, 1931.

Clauer, C. R. and R. L. McPherron, Mapping the local time-universal time development of magnetospheric substorms using mid-latitude magnetic observations, *J. Geophys. Res.*, *79*, 2811, 1974.

Dessler, A. J. and R. D. Juday, Configuration of auroral radiation in space, *Planet. Space Sci.*, *13*, 63, 1965.

Dungey, J. W., Conditions for the occurrence of electrical discharges in astrophysical systems, *Phil. Mag.*, *44*, 725, 1953.

Dungey, J. W., Interplanetary magnetic field and the auroral zones, *Phys. Rev. Lett.*, *6*, 47, 1961.

Frank, L. A. and K. L. Ackerson, Observations of charged particle precipitation into the auroral zone, *J. Geophys. Res.*, *76*, 3612, 1971.

Fukushima, N., Polar magnetic storms and geomagnetic bays, *J. Fac. Sci., Tokyo Univ.*, *8*, 293, 1953.

Fukushima, N. and Y. Kamide, Partial ring current models for world geomagnetic disturbances, [illegible], [illegible], 795, 1973.

Hones, E. W., Jr., J. R. Asbridge, S. J. Bame and S. Singer, Substorm variations of the magnetotail plasma sheet from $X_{SM} \approx -6R_E$ to $X_{SM} \approx -60R_E$, [illegible], [illegible], 109, 1973.

Iijima, T. and T. Nagata, Signatures for substorm development of the growth phase and expansion phase, [illegible], [illegible], 1095, 1972.

Kamide, Y. and N. Fukushima, Positive geomagnetic bays in evening high-latitudes and their possible connection with partial ring current, [illegible], [illegible], 79, 1972.

Kellogg, P. J., Flow of plasma around the earth, [illegible], [illegible], 3805, 1962.

Kisabeth, J. L., The dynamical development of the polar electrojets, Ph.D. Thesis, Univ. of Alberta, Fall, 1972.

Kisabeth, J. L. and G. Rostoker, Current flow in auroral loops and surges inferred from ground-based magnetic observations, J. Geophys. Res., [illegible], 5573, 1973.

Kisabeth, J. L. and G. Rostoker, The expansive phase of magnetospheric substorms, I, Development of the auroral electrojets and auroral arc configuration during a substorm, J. Geophys. Res., 79, 972, 1974.

Kokubun, S., Relationship of interplanetary magnetic field structure with development of substorm and storm main phase, Planet. Space Sci., 20, 1033, 1972.

Lezniak, T. W. and J. R. Winckler, Experimental study of magnetospheric motions and the acceleration of energetic electrons during substorms, J. Geophys. Res., 75, 7075, 1970.

McPherron, R. L., Growth phase of magnetospheric substorms, J. Geophys. Res., 75, 5592, 1970.

McPherron, R. L., Substorm related changes in the geomagnetic tail: the growth phase, [illegible] 20, 1521, 1972.

McPherron, R. L., C. T. Russell and M. P. Aubry, Satellite studies of magnetospheric substorms on August 15, 1968, 9. Phenomenological model for substorms, [illegible], 3131, 1973.

McPherron, R. L., Critical problems in establishing the morphology of substorms in space, in: Magnetospheric Physics, ed. by B. M. McCormac, p. 335, D. Reidel Publ. Co., Dordrecht-Holland, 1974.

Ness, N. F., K. W. Behannon, S. C. Cantarano and C. S. Scearce, Observations of the earth's magnetic tail and neutral sheet at 510,000 kilometers by Explorer 33, [illegible], 927, 1967a.

Ness, N. F., C. S. Scearce and S. Cantarano, Probable observation of the geomagnetic tail at 10^3 R_E by Pioneer 7, [illegible], 3769, 1967b.

Ness, N. F., The geomagnetic tail, [illegible], 97, 1969.

Nishida, A., Formation of plasmapause by the combined action of magnetospheric convection and plasma escape from the tail, [illegible], 71, 5669, 1966.

Petschek, H. E., Magnetic field annihilation, NASA SP-50, Proceedings of AAS-NASA Symposium on the Physics of Solar Flares, ed. by W. N. Hess, p. 425, 1964.

Piddington, J. H., Geomagnetic storm theory, [illegible], 93, 1960.

Piddington, J. H., A hydromagnetic theory of geomagnetic storms and auroras, [illegible], 947, 1962.

Ratcliffe, J. A., An Introduction to the Ionosphere and Magnetosphere, Cambridge University Press, 1972.

Rostoker, G. and F. P. Camidge, Localized character of magnetotail magnetic fluctuations during polar magnetic substorms, *J. Geophys. Res.*, *76*, 6944, 1971.

Rostoker, G., Current flow in the magnetosphere during magnetospheric substorms, *J. Geophys. Res.*, *79*, 1994, 1974.

Rostoker, G. and R. Boström, A mechanism for driving the gross Birkeland current configuration in the auroral oval, *J. Geophys. Res.*, *81*, 235, 1976.

Sergeev, V. A., On localization and spreading of particle precipitation region during the magnetospheric substorm, *IAGA Bulletin 34*, 458, 1973.

Spreiter, J. R. and A. Y. Alkshe, Effect of the neutral sheet currents on the shape and magnetic field of the magnetosphere tail, *Planet. Space Sci.*, *17*, 233, 1969.

Van Allen, J. A., Absence of 40-kev electrons in the earth's magnetospheric tail at 3300 earth radii, *J. Geophys. Res.*, *70*, 473, 1965.

Vorobiev, V. G. and B. V. Rezhenov, Progressive westward displacements of the region of the auroral substorm localization in conjunction with impulsive variations of the magnetic field, *IAGA Bulletin*, *34*, 441, 1973.

Wiens, R. G. and G. Rostoker, Ground based magnetic signatures of the phases of magnetospheric substorms - a reconciliation, *EOS, Trans. Amer. Geophys. Union*, *54*, 412, 1973.

Wiens, R. G. and G. Rostoker, Characteristics of the development of the westward electrojet during the expansive phase of magnetospheric substorms, *J. Geophys. Res.*, *80*, 2109, 1975.